

AD-A058 509

NAVAL POSTGRADUATE SCHOOL MONTEREY CALIF

F/G 8/3

FINESTRUCTURE, FRONTS AND CURRENTS IN THE PACIFIC MARGINAL SEA--ETC(U)

JUN 78 G P GRAHAM, R G PAQUETTE, R H BOURKE

UNCLASSIFIED

NPS68-78-006

NL

1 OF  
AD  
A058509



END

DATE

FILMED

11-78

DDC

AD No. ADA 058509  
DDC FILE COPY

NPS 68-78-006

(2)

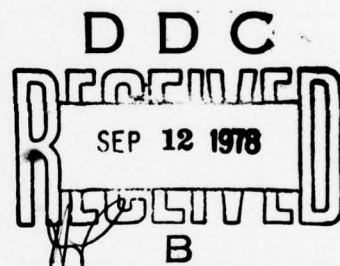
LEVEL *II*

# NAVAL POSTGRADUATE SCHOOL

## Monterey, California



# THESIS



FINESTRUCTURE, FRONTS AND CURRENTS IN THE  
PACIFIC MARGINAL SEA-ICE ZONE -  
MIZPAC 77

by

Gordon Patrick Graham

June 1978

Thesis Advisors:

R. G. Paquette  
R. H. Bourke

Approved for public release; distribution unlimited.

A report submitted to:  
Director, Arctic Submarine Laboratory  
Naval Ocean Systems Center, San Diego

78 08 14 070

NAVAL POSTGRADUATE SCHOOL  
Monterey, California

Rear Admiral T. F. Dedman  
Superintendent

Jack R. Borsting  
Provost

This thesis is prepared in conjunction with research  
supported in part by the Arctic Submarine Laboratory,  
Naval Ocean Systems Center, San Diego, California under  
Project Order Nos. 00610 and 00002.

Reproduction of all or part of this report is authorized.

Released as a Technical Report by:

William M. Toller  
\_\_\_\_\_  
Dean of Research (Acting)

UNCLASSIFIED

SECURITY CLASSIFICATION OF THIS PAGE (When Data Entered)

REPORT DOCUMENTATION PAGE		READ INSTRUCTIONS BEFORE COMPLETING FORM
1. REPORT NUMBER NPS 68-78-006	2. GOVT ACCESSION NO. DN89440	3. RECIPIENT'S CATALOG NUMBER
4. TITLE (If Subtitle) Finestucture, Fronts and Currents in the Pacific Marginal Sea-Ice Zone - MIZPAC 77		5. TYPE OF REPORT & PERIOD COVERED INTERIM 1 July 77 - 30 JUNE 78
6. AUTHOR(s) Gordon P. Graham in conjunction with Robert G. Paquette and Robert H. Bourke		7. PERFORMING ORGANIZATION NAME AND ADDRESS Naval Postgraduate School Monterey, California 93940
8. CONTROLLING OFFICE NAME AND ADDRESS Arctic Submarine Laboratory Code 54, Bldg 371, Naval Ocean Syst. Ctr San Diego, California 92152		9. PROGRAM ELEMENT, PROJECT, TASK AREA & WORK UNIT NUMBERS Element: 627759N; Work: 9024909; Project: F52-555; Task: 7F52-555-01Z
10. MONITORING AGENCY NAME & ADDRESS (if different from Controlling Office) F52555		11. REPORT DATE June 1978
		12. NUMBER OF PAGES 88
		13. SECURITY CLASS. (of this report) Unclassified
		14. DECLASSIFICATION/DOWNGRADING SCHEDULE
15. DISTRIBUTION STATEMENT (of this Report) Approved for public release; distribution unlimited.		
16. DISTRIBUTION STATEMENT (of the abstract entered in Block 20, if different from Report) 9 Interim Rept. 1 Jul 77-30 Jun 78		
17. SUPPLEMENTARY NOTES 10 Gordon Patrick /Graham, Robert G. /Paquette Robert H. /Bourke		
18. KEY WORDS (Continue on reverse side if necessary and identify by block number) Marginal Sea-ice Zone MIZPAC Microstructure Thermal Finestucture CTD Fronts Chukchi Sea Salinity Spiking Currents Arctic Ocean Oceanography		
19. ABSTRACT (Continue on reverse side if necessary and identify by block number) Sharp vertical temperature fronts and complex temperature inversions observed in the Chukchi Sea during MIZPAC 77 were investigated in a further effort to define the mechanisms for the formation of finestucture. An association was found between the upper level current directions inferred from the gross ice edge recession rates and the occurrence of fronts and finestucture. Currents with a		

Unclassified

SECURITY CLASSIFICATION OF THIS PAGE/When Data Entered.

strong directional component normal to the ice edge were associated with extensive finestructure and those with a weak component were associated with sharp fronts but little or no finestructure. Six closely spaced crossings of the Alaskan Coastal Current made it possible to describe the circulation in greater detail than was previously possible. A peculiar ice bay was discovered off Point Barrow in which there was extensive finestructure, including some which was deeper than any previously observed.

AX		
NTIS		
DDC		
CDR		
JULY 1973		
BY		
DISTRIBUTION BY COUNTRY		
Dist.		
SPECIAL		
A		

DD Form 1473  
1 Jan '3  
S/N 0102-014-6601

Unclassified  
SECURITY CLASSIFICATION OF THIS PAGE/When Data Entered)

Approved for public release; distribution unlimited.

Finestructure, Fronts and Currents in the  
Pacific Marginal Sea-Ice Zone -  
MIZPAC 77

by

Gordon Patrick Graham  
Lieutenant Commander, Canadian Armed Forces  
B.S., University of Victoria, 1969

Submitted in partial fulfillment of the  
requirements for the degree of

MASTER OF SCIENCE IN OCEANOGRAPHY

from the  
NAVAL POSTGRADUATE SCHOOL  
June 1978

Author

Gordon P. Graham

Approved by:

Robert A. Paquette

Thesis Advisor

Robert A. Bourke

Thesis Advisor

Dale F. Leibner

Chairman, Department of Oceanography

G. J. Haltiner

Dean of Science and Engineering

## ABSTRACT

Sharp vertical temperature fronts and complex temperature inversions observed in the Chukchi Sea during MIZPAC 77 were investigated in a further effort to define the mechanisms for the formation of finestructure. An association was found between the upper level current directions inferred from the gross ice edge recession rates and the occurrence of fronts and finestructure. Currents with a strong directional component normal to the ice edge were associated with extensive finestructure and those with a weak component were associated with sharp fronts but little or no finestructure. Six closely spaced crossings of the Alaskan Coastal Current made it possible to describe the circulation in greater detail than was previously possible. A peculiar ice bay was discovered off Point Barrow in which there was extensive finestructure, including some what was deeper than any previously observed.

PRECEDING PAGE BLANK-NOT FILMED

## TABLE OF CONTENTS

I.	INTRODUCTION	12
	A. BACKGROUND	12
	B. MIZPAC 77	15
II.	EQUIPMENT AND TECHNIQUES	17
	A. CONDUCTIVITY-TEMPERATURE-DEPTH RECORDER (CTD)	17
	B. NANSEN CASTS	18
	C. CURRENT METER	18
III.	DATA REDUCTION AND DISPLAY	19
	A. ERROR ANALYSIS	19
	1. Depth	19
	2. Temperature	19
	3. Salinity	19
	4. Despiking	21
	B. CALCULATIONS AND DISPLAY	21
	1. Sigma-t (ST) and Sound Speed (SV)	21
	2. Dynamic Heights	22
IV.	ANALYSIS	23
	A. WATER MASS AREAS	23
	1. The Northern Area	23
	2. The Southern Area	24
	3. The Transition Zone	25
	B. TEMPERATURE FRONTS	26
	1. Cross-section No. 1	27

2. Cross-sections Nos. 2, 3, and 4	27
3. Cross-section No. 5	29
C. FINESTRUCTURE	30
1. Definition and Classification	30
2. Distribution during MIZPAC 77	31
3. Formation	34
4. Finestructure Element Extent	34
D. THE ALASKAN COASTAL CURRENT	36
E. UPPER LEVEL CURRENTS	37
V. DISCUSSION	41
A. MIZPAC 77	41
1. Point A	41
2. Point B	42
3. Point C	43
B. MIZPAC 71	44
C. MIZPAC 72	44
D. MIZPAC 74	45
E. MIZPAC 75	46
VI. CONCLUSIONS	48
FIGURES	50
BIBLIOGRAPHY	81
INITIAL DISTRIBUTION LIST	83

LIST OF TABLES

TABLE I.	MIZPAC 77 Cruise Summary	16
TABLE II.	Error Analysis Summary	20
TABLE III.	MIZPAC 77 Finestructure Classification System	32

## LIST OF FIGURES

FIGURE	PAGE
1. Property profiles for a station showing strong finestructure	50
2. MIZPAC 77 station plot	51
3. Property profiles of a representative station in the northern area	52
4. Property profiles of a representative station in the southern area	53
5. Temperature and salinity cross-section No. 1	54
6. Temperature and salinity cross-section No. 2	55
7. Temperature and salinity cross-section No. 3	56
8. Temperature and salinity cross-section No. 4	57
9. Temperature and salinity cross-section No. 5	58
10. Property profiles for a station showing a "nose" with finestructure	59
11. Property profiles for a station showing a "nose" without finestructure	60
12. Distribution and intensity of fine-structure during MIZPAC 77	61
13. Temperature and salinity cross-section No. 6	62
14. Temperature and salinity cross-section No. 7A	63
15. Temperature and salinity cross-section No. 7B	64
16. Temperature and salinity cross-section No. 8	65
17. Property profiles of stations in the ice bay off Point Barrow	66
18. Schematic of a portion of a vertical density cross-section	67

FIGURE	PAGE
19. Temperature and salinity cross-section No. 9	68
20. Temperature and salinity cross-section No. 10	69
21. Temperature and salinity cross-section No. 11	70
22. Temperature and salinity cross-section No. 12	71
23. Temperature and salinity cross-section No. 13	72
24. Temperature and salinity cross-section No. 14	73
25. Upper level currents in the Chukchi Sea as inferred from gross ice edge recession rates from 12 July to 3 August 77	74
26. Chart of MIZPAC 77 surface dynamic heights referenced to 40 m	75
27. Surface dynamic heights referenced to 40 m for 2/3 August 77 around Point C	76
28. Distribution and intensity of fine- structure for MIZPAC 71	77
29. Distribution and intensity of fine- structure for MIZPAC 72	78
30. Distribution and intensity of fine- structure for MIZPAC 74	79
31. Distribution and intensity of fine- structure for MIZPAC 75	80

#### ACKNOWLEDGEMENT

I wish to express my gratitude to the faculty and staff of the Naval Postgraduate School for their help and guidance throughout my graduate studies. I am especially grateful to Drs. R. G. Paquette and R. H. Bourke. Their interest and patience were invaluable in the preparation of this thesis.

## I. INTRODUCTION

### A. BACKGROUND

In the Chukchi Sea during the melt season, oceanographic phenomena have been identified which differ from those found anywhere in the oceans. In the Marginal Sea-Ice Zone Pacific (MIZPAC), temperature fronts have been discovered with horizontal gradients as strong as  $2^{\circ}\text{C}/\text{km}$ . In the same area, extensive temperature finestructure has been found with peak-to-peak fluctuations often exceeding  $2^{\circ}\text{C}$ . An example of this finestructure can be seen in Figure 1. The sound speed (SV) profile in Figure 1 hints at the effect that finestructure has on sound propagation in the vicinity of the ice edge. This effect has made finestructure an operational as well as a scientific concern.

The phenomenon of temperature finestructure near the ice edge was first observed in NEREUS 1947 bathythermograph records, and was reported by LaFond and Pritchard in 1952. After that, little extensive study appears to have been made until PROJECT MIZPAC was established by the Arctic Submarine Laboratory, Naval Ocean Systems Center, San Diego, California. The overall purpose of this project was to develop arctic submarine technology and to enhance the understanding of the complex sound speed profiles and rapid changes in propagation conditions with distance in the MIZPAC area.

As part of the MIZPAC program, personnel from the Naval Postgraduate School (NPS) have taken part in cruises to the ice edge in 1971, 72, 74, 75 and 77. The object of these cruises was to investigate the oceanographic processes which cause and modify the complex structure found near the ice in the Chukchi Sea. Initial results of MIZPAC 71 and 72 were reported by Garrison and Pence (1973) and Paquette and Bourke (1973). The latter two authors described the temperature phenomena near the ice edge and the two layered structure south of the ice. As well, Paquette and Bourke (1974) described the Alaska Coastal Current, its descent into mid-depth along the continental slope and its intrusion into the Beaufort Sea.

Corse (1974) examined MIZPAC 71 data with respect to finestructure formation and its space-time distribution. He found a correlation between finestructure elements in a time series over a period of several hours. He suggested that there might be a correlation between internal waves and the type of finestructure.

Karrer (1975) examined MIZPAC 74 data. He made heat and ice-melt evaluations in the vicinity of the ice edge and hypothesized that the local dynamic height gradient near the ice edge was a possible driving force for downward mixing. Paquette and Bourke (1976) re-evaluated Karrer's analysis and suggested that finestructure might be formed by lateral mixing of southerly and northerly waters having nearly the same density but different temperatures. They reported that

strong finestructure was associated with rapid melting and rapid flow of warm water toward the ice. They also noted that Bering Sea water appeared to move northward at about the same rate as the ice margin retreated.

Zuberbuhler and Roeder (1976) reported on the MIZPAC 75 cruise. They discovered temperature fronts at the ice edge. As well, they analyzed currents and time series measurements taken during MIZPAC 75. They attempted to find an association between finestructure and directly measured currents, but their conclusions are suspect because of subsequently discovered serious effects of the ship's magnetism on the compass in the current meter.

Handlers (1977) studied aspects of a melt-water zone and the correlation on the water flow rate with the rate of ice retreat. He suggested that the surface currents flow faster than the ice retreats during the summer in the eastern half of the Chukchi Sea.

Bourke and Paquette (1977) evaluated the effects of finestructure on acoustic propagation in the MIZPAC area. They found that propagation conditions could be regionally categorized with respect to distance from the ice edge. Paquette and Bourke (1978b) summarized the knowledge gained in MIZPAC 71, 72, 74 and 75. They discussed finestructure categorization, distribution, persistence and causes. They described the temperature fronts found at the ice edge and suggested that the fronts are associated with the flow regimes of the warm water currents in the Chukchi Sea. They also suggested

that local lateral pressure gradients might be the driving force for the formation of finestructure. A summary of the data collected during the MIZPAC 77 cruise was reported by Paquette and Bourke (1978a).

#### B. MIZPAC 77

The MIZPAC 77 cruise was undertaken aboard USCGC BURTON ISLAND from 24 July to 6 August 77. The primary objective of the cruise was to find and characterize finestructure in the vertical temperature profiles and to discover its horizontal distribution and causes. Stations were occupied in the positions indicated in Figure 2. The ice edge depicted in Figure 2 is not synoptic but is constructed from the position of the ice edge at the time of each station that was taken within sight of the ice edge. The positions marked as Point A, B and C in Figure 2 are locations of phenomena of special interest and will be described in subsequent sections of this thesis.

Table I is a summary of some of the significant information pertaining to the MIZPAC 77 cruise.

Considerable finestructure was discovered during the MIZPAC 77 cruise, some of it deeper than any previously seen. In addition, the most striking temperature fronts yet noted were found at the ice edge. The main thrust of the analysis in this thesis is an attempt to explain why fronts are found at some places along the ice edge while finestructure is found at others. An association will be suggested between current patterns, ice edge retreat rates and the occurrence of fronts and finestructure.

TABLE I  
MIZPAC 77 CRUISE SUMMARY

EMBARKATION: 24 July at Nome, Alaska  
DEBARKATION: 6 August at Point Barrow, Alaska  
OPERATION PLATFORMS: USCGC BURTON ISLAND and her helicopters  
OCEANOGRAPHIC EQUIPMENT: 1. Two lightweight CTD systems from the Applied Physics Laboratory, University of Washington.  
2. Nansen bottles and reversing thermometers.  
NAVIGATION SYSTEMS: Loran/Omega/Radar/Visual  
STATIONS OCCUPIED: 157  
STATIONS WITH CTD DIGITAL OUTPUT: 150  
NANSEN CASTS: 50  
SCIENTIFIC PARTY: Dr. Robert G. Paquette,  
NPS, Chief Scientist  
Dr. Robert H. Bourke, NPS  
LCDR Gordon P. Graham, Canadian Armed Forces, Student at NPS  
Mr. Jonathan D. Trent, NPS  
Mr. Peter Becker, APL-UW, Seattle

## II. EQUIPMENT AND TECHNIQUES

### A. CONDUCTIVITY-TEMPERATURE-DEPTH RECORDER (CTD)

The primary instrument used to gather data during the MIZPAC 77 cruise was a hand-lowered CTD developed by the Applied Physics Laboratory, University of Washington (APL-UW) (Pederson, 1973). Data were recorded digitally on a cassette tape mounted on the winch drum. A lowering rate of approximately 1 m/sec was used, resulting in a data rate of 3 points/m. Before leaving station, the CTD data were plotted utilizing a Hewlett/Packard 9100 series computer/plotter system. Using this technique the scientist taking the cast could ensure that good data had been recorded and could also decide on future courses of action based on the findings of each station.

Eighteen stations were occupied by lowering the CTD from a hovering helicopter. The same plotting procedure was followed as soon after the flight as possible. The utility of onboard plotting was shown when it was found by this technique that the CTD had failed to function properly on one flight. Between the ship and the helicopters, a total of 157 stations were occupied and 150 of them provided usable data.

After the cruise, the cassette tapes were taken to APL-UW where the data were transferred to a 7-track tape and forwarded to NPS for editing and analysis.

## B. NANSEN CASTS

Standardizations of the CTD were accomplished with a total of 50 casts made with a Nansen bottle 2 to 5 m above the sea floor. It was expected that this depth would place the bottle in a portion of the water column which frequently is constant in temperature and salinity. This technique proved to be successful, as 49 samples were found to have been positioned in an isothermal layer and 40 in an isohaline layer. Positioning the sample bottle in such layers was necessary to avoid errors due to depth uncertainties and non-simultaneity between the CTD and the Nansen bottle.

## C. CURRENT METER

Current speed and direction were to be measured with a profiling current meter. However, such measurements were omitted because of difficulties with the magnetic direction sensor due to a destructive distortion of the earth's magnetic field by the ship's iron, even at 40 m depth.

### III. DATA REDUCTION AND DISPLAY

#### A. ERROR ANALYSIS AND CORRECTION

##### 1. Depth

The CTD depth sensor had been calibrated assuming a specific density of 1.00. Consequently, all depth values in salt water were too large. In order to remove this error, depth data were divided by a mean sea water density of 1.025.

##### 2. Temperature

The temperature of the water near the bottom was determined at 50 stations using standard reversing thermometers, and these values were used as the standards for error analysis. CTD errors were plotted versus time to find outliers and to determine if there was a systematic drift. One outlier was found and set aside. Further investigation indicated a probable recording error in the reversing thermometer data at that station. No systematic drift was found and the other 49 data points were used to calculate the statistics summarized in Table II. The raw CTD temperatures were subsequently corrected using the tabulated mean error correction.

##### 3. Salinity

Water samples from near the bottom were taken at the same 50 stations used for temperature, and the salinity was determined using a portable laboratory salinometer. As with

TABLE II  
MIZPAC 77 ERROR ANALYSIS SUMMARY

	<u>TEMPERATURE</u>	<u>SALINITY</u>
NUMBER OF POINTS - - - - -	49	40
MEAN ERROR CORRECTION - - - - (NANSEN - CTD)	-0.078°C	+0.021 °/oo
STANDARD DEVIATION - - - - -	<u>±0.036°C</u>	<u>±0.025 °/oo</u>
STANDARD ERROR OF THE MEAN - -	<u>±0.0051</u>	<u>±0.0040</u>

temperature, the CTD salinity errors were plotted versus time to find outliers and to determine if there was a systematic drift. Ten outlying data points were found and were set aside because the salinity near these points was changing rapidly with depth. No systematic drift was found, and the remaining 40 points were used to calculate the salinity statistics summarized in Table II. The salinity values, despiked as described below, were corrected using the tabulated mean error correction.

#### 4. Despiking

Because the response time constants of the temperature and salinity errors were different and because of a physical time lag between the measurements of conductivity and temperature, rapidly changing temperatures caused anomalous spikes to appear in the salinity traces. The situation was further complicated by the presence of an additional long time constant in the conductivity response which was apparently due to heat storage in the cell structure. These effects were corrected by a computerized calculation. A detailed description of the despiking and editing routines has been reported by Paquette and Bourke (1978a).

### B. CALCULATIONS AND DISPLAY

#### 1. Sigma-t (ST) and Sound Speed (SV)

Using the corrected values of salinity, temperature and depth, values of sigma-t and sound speed were calculated by computer. Plots of T, S, ST and SV versus depth were subsequently produced. Examples of these plots are displayed

as in Figures 1, 3, 4 and 17. The complete set has been published in the MIZPAC 77 data report by Paquette and Bourke (1978a). Temperature and salinity values have been used in this thesis, but because of the number of diagrams involved, sigma-t and sound speed have not.

## 2. Dynamic Heights

From the corrected depth, temperature and salinity values, the dynamic height of the sea surface was calculated for each station. This was accomplished by integrating the specific volume anomaly from 40 m to the surface. Since the depth was so shallow, pressure effects were ignored and the anomaly was determined only from the salinity and temperature.

#### IV. ANALYSIS

##### A. WATER MASS AREAS

As an aid to understanding the processes which take place during the melt season, the Chukchi Sea will be divided into three areas based on an analysis of the water masses present during the summer. Two of these areas contain water with reasonably consistent temperature and salinity profiles. The third area lies between the other two and contains a variety of profiles. These areas are not geographically stationary, so they are defined with respect to the ice edge. The stations used for examples will be from MIZPAC 77, but the general definitions will be valid for any year.

###### 1. The Northern Area

The first area to be considered will be called the northern area. It includes all of the Chukchi Sea that is covered with ice except the portion within a few kilometers of the ice edge.

A plot of the property profiles for a representative station in the northern area is included in Figure 3. In the northern area during the melt season, there is an upper and a lower layer. The lower layer extends from the sea floor to within a few meters of the surface. Possible secondary layering within this layer is not discussed. The maximum salinities in this layer vary between 33.0 and 33.8 ‰. The temperatures in the lower layer are

consistently cold. They vary between  $-1.6^{\circ}$  and  $-1.8^{\circ}\text{C}$ . As the water in this layer is close to its equilibrium freezing temperature, it is likely relict water from the last year's freezing.

The upper layer is separated from the lower layer by a sharp halocline 2 to 10 m from the surface. The salinities in this layer vary greatly from station to station, but are always much less than in the lower layer, usually less than 28 ‰. The low salinity of the upper layer is clearly a result of the melting of the ice above it, so the thickness of the layer and its salinity vary with the rate of melting and vertical mixing. Its temperatures vary with the rates of insolation and mixing, but are usually between  $-1^{\circ}$  and  $0^{\circ}\text{C}$ .

Because of the density contrast between the two layers, there is little or no vertical mixing through the halocline and the heat of insolation is confined to the upper layer. A consequence is that the lower layer stays very cold unless heat is supplied horizontally.

Henceforth, water from the northern area will be referred to simply as northern water.

## 2. The Southern Area

The next area to be considered will be called the southern area. It includes all of the Chukchi Sea from which all evidence of the ice and of the northern water have been removed by warm currents and protracted insolation. Its northern boundary varies from a few km to more than 125 km

outside the ice. A plot of property profiles for a representative station in the southern area is included as Figure 4.

The water in the southern area has complex origins (Coachman et al., 1975), but when it has reached the eastern Chukchi Sea its characteristics have become fairly consistent. The dominant contributor to the southern water in the MIZPAC area is Alaskan Coastal Water. It flows northward from Bering Strait, turns in toward Kotzebue Sound where it is reinforced with a warm, low-salinity contribution and thence northward past Point Hope. North of Bering Strait the water rapidly becomes stratified with a sharp thermocline at approximately 20 m which separates the water column into an upper and a lower layer. The lower layer has minimum temperature of about  $2^{\circ}\text{C}$ . The upper layer, which has been warmed by insolation, has maximum temperatures as high as  $10^{\circ}\text{C}$ .

Salinities vary from location to location and from year to year, but they are generally between 31 ‰ and 33 ‰. Salinities do not vary greatly from the surface to the sea floor at any given station.

Henceforth, water from the southern area will be referred to simply as southern water.

### 3. The Transition Zone

In this thesis, the transition zone will be defined simply as the area between the well-defined northern and southern areas. In this definition, the idea of a transition

is used to indicate that there is a progressive change in properties in a horizontal direction between the two previously defined water masses. The width of the transition zone will be considered as the distance from the southern area to the northern area. The width will be shown later to vary from as little as a few km to as much as 125 km.

Contrary to what one might expect, the northern boundary of the transition zone is not always at, or very close to the ice margin. It usually extends up to 10 km into the ice pack, to a point where there is little further decrease in temperature northward at any depth. The northern boundary is not geographically fixed, but moves with the ice. The southern boundary apparently also is related to the ice margin, but its position relative to the ice varies much more than does that of the northern boundary.

Profiles of temperature and salinity vary greatly in the transition zone. It is in this area that fronts and finestructure are found; hence this region will be the subject of most of the subsequent discussion.

#### B. TEMPERATURE FRONTS

Some of the most striking features that have been found in the MIZPAC transition zone are temperature fronts. At the water temperatures found in the MIZPAC area, the salinity dominates the density. Therefore, water parcels of different temperatures but the same salinity can be at the same depth without causing dynamic imbalances. Fronts of considerable sharpness are found, some having horizontal gradients up to

$2^{\circ}\text{C}/\text{km}$ . In contrast, maximum horizontal gradients of  $0.3^{\circ}\text{C}/\text{km}$  at the eastern edge of the Kuroshio Current were reported by Cheney (1977). The various frontal characteristics can best be demonstrated by transects normal to the ice edge. Such crossings normally encompass all three water mass areas. Five cross-sections, illustrating various frontal features, are described below. The location of each cross-section can be seen in Figure 2.

#### 1. Cross-section No. 1

Figure 5 shows a temperature front which extends from the surface to the sea floor. It represents the position where the transition zone was the narrowest found during the MIZPAC 77 cruise. During MIZPAC 75 (Zuberbuhler and Roeder, 1976), two fronts which extended from the surface to the sea floor were discovered within 15 km of the position of the front in Figure 5 of 1977. In no other MIZPAC data to date does this phenomenon appear so clearly. This suggests, then, that there is something about this geographical location which allows fronts, which extend from the surface to the sea floor, to form. A further study of this location will be made in Section V, where it will be examined with respect to upper level currents and movements of the ice edge. This location is marked as Point A on Figures 2, 25 and 26.

#### 2. Cross-sections Nos. 2, 3 and 4

Figures 6, 7 and 8 are temperature and salinity cross-sections Nos. 2, 3 and 4. From the surface to approximately 20 m they show temperature fronts, at the ice edge, which

resemble the near surface portions of the front in cross-section No. 1. The water on the warm side of the front has the characteristics of the water found in the southern area while the water on the cold side has the characteristics of water found in the northern area. However, below approximately 20 m all of the water in cross-sections 2, 3 and 4 has the properties which would normally be found in the lower layer in the northern area. This phenomenon of southern water overlying apparently unaltered northern water has not been found in any of the previous MIZPAC cruises. Of course, the cruises are of limited duration and do not cover the whole transition zone. Therefore, there may have been features of this type which were not encountered.

As can be seen in Figure 2, all of these cross-sections are in the same general area, near Point B. They were measured over a period of 7 days, which suggests that the conditions for the existence of this two-layered phenomenon persisted for at least a week. Two possible mechanisms were considered for the formation of this layering. One possibility was that there had been, further south, a front which extended from the surface to the sea floor, much like the front in cross-section No. 1. Winds might have pushed the ice and the surface water farther north where a new front was formed in the upper layer. However, no significant storms were noted in the area in the period immediately preceding the data being taken. Therefore, this mechanism was not considered the most likely.

The second possibility is that the upper layer of southern water had simply moved into the area while the lower layer had not. An examination of historical current measurements tends to support this view. Current measurements made in the MIZPAC area by the BROWN BEAR in 1960, by the STATEN ISLAND in 1968, during WEBSEC 70 and by the OSHORO MARU in 1972 have been reported by Coachman et al. (1975). Also, measurements were made during MIZPAC 75 and were reported by Zuberbuhler and Roeder (1976). These measurements are difficult to interpret for direction, but they are quite consistent in indicating higher speeds near the surface than near the sea floor. An analysis of current speeds was made by Handlers (1977) which indicates that the currents in the upper 10 m of the water column travel 15 to 50 per cent faster than the currents in the deeper levels. As added evidence, it should be noted that the thermocline in the southern area is at approximately 20 m, the same depth as the thermoclines in cross-sections 2, 3 and 4. Therefore, it is likely that the two-layered phenomenon seen in Figures 6, 7 and 8 is caused by the upper layer current from the southern area flowing over the lower layer water in a portion of what had previously been the northern area.

### 3. Cross-section No. 5

Figure 9 shows temperature and salinity cross-section No. 5. This cross-section shows some of the same characteristics as cross-sections 2, 3 and 4. It has a front which extends down to 30 m with southern water on one side and

northern water on the other. As well, it has a sharp thermocline on the warm side of the front. This cross-section differs from cross-sections 2, 3 and 4 in that the water below the thermocline is not unaltered northern lower layer water. In this, it is more similar to the cross-sections found in the previous MIZPAC cruises. Cross-section 5 is not far from cross-sections 2, 3 and 4 and it is not clear why the water below the thermocline is not the same throughout the area. One possible explanation is that there are different dynamics operating at the position of cross-section 5. This is evidenced by an ice tongue at that location.

#### C. FINESTRUCTURE

##### 1. Definition and Classification

Finestucture, previously referred to as mesostructure, has been defined in a variety of ways. In this thesis, the method followed will be from that of Paquette and Bourke (1978b). Finestucture is characterized by significant property inversions over a small vertical extent. In the case of interest here, the property is temperature with inflections frequently of  $1^{\circ}$  or  $2^{\circ}\text{C}$  over a vertical extent of the order of a few meters. Examples of this structure can be seen in Figures 1 and 13. Another significant feature which has been found during MIZPAC cruises is called a "nose". This phenomenon is a near-surface temperature maximum with a vertical extent usually larger than finestucture. A nose may have finestucture embedded in it, but need not. An example of a nose with finestucture can be seen in Figure 10 and one without in Figure 11.

The categorization scheme from Paquette and Bourke (1978b) is displayed as Table III and a chart illustrating the distribution of the finestructure found during the MIZPAC 77 cruise is shown in Figure 12. Included in Figure 12 are isotherms of the maximum temperature in the water column. They are used as a visual aid in inferring current directions later in this thesis.

## 2. Distribution during MIZPAC 77

All finestructure that has been found during this and previous MIZPAC cruises has been in the transition zone. However, finestructure is not present everywhere in the zone. Rather, it is locally concentrated. Paquette and Bourke (1976) have indicated that finestructure is found most often in areas of active melting which is caused by rapid heat flow toward the ice.

It can be seen from Figure 12 that there was a definite geographical pattern to the finestructure found during MIZPAC 77. In the most westerly of the areas visited during this cruise, very little finestructure was seen. However, as stations were taken more to the east, the structure became stronger and more prevalent. In the ice bay off Point Barrow, almost every station showed at least moderate structure. Cross-sections 6, 7A, 7B and 8 were drawn through this bay and are included as Figures 13 to 16. Cross-section 6 is directed east-west while the others are north-south. These cross-sections indicate an area with complex temperature patterns. Although the ice bay was well covered with stations, little continuity of finestructure

TABLE III  
MIZPAC 77 FINESTRUCTURE CLASSIFICATION SYSTEM

<u>SYMBOL</u>	<u>CATEGORY</u>	<u>FLUCTUATION AMPLITUDE</u>
Circle with dot	Weak	0.2 to 0.5 deg C
Circle with cross	Moderate	0.5 to 1.0 deg C
Solid circle	Strong	More than 1.0 deg C
Open tab on circle	Nose without structure	
Closed tab on circle	Nose with structure	

elements could be discerned in any direction. As well, there was no discernible pattern to the finestructure intensities. This suggests that there is a very complex flow regime in the ice bay.

In past MIZPAC cruises, few instances have been found of finestructure below 30 m depth, and when it has been found it has been weak. Paquette and Bourke (1978b) suggested that the rarity of such deep structure might be associated with a lack of sufficient warmth at these depths to create significant temperature inflections. However, of the 70 stations taken inside the ice bay off Point Barrow during MIZPAC 77, 29 showed finestructure below 30 m. Examples of some of this deeper finestructure can be seen in Figure 17. The stations in Figure 17 were in the north-eastern part of the ice bay on the north slope of the Barrow Canyon in an area with depths of approximately 70 m. Station 101 was taken inside the ice and showed no finestructure and Station 102 shows only weak structure below 30 m, much as in past MIZPAC data. On the other hand, Stations 99 and 100 have moderate structure as deep as 50 m. It appears that water masses of significantly different temperatures were interleaving even as deep as 50 m, and that the heat was available at that depth to allow for strong temperature gradients.

It should be noted that the colder of the deep interleaving waters at Stations 99 and 100 had the right temperature and salinity for resident northern water. These stations were obviously taken after interleaving had commenced but

before the resident northern water had had a chance to be warmed. It appears that the warming of the deeper water in this area had only recently commenced although the ice above it had been gone for several days.

### 3. Formation

In the vicinity of the ice edge in the Chukchi Sea, water parcels of different temperatures but similar densities are in close horizontal proximity at the same depth. The situation is manifested by the temperature fronts previously shown in Figures 5 to 9. It is not surprising, then, that these waters will interleave along equal density lines if an appropriate driving force is applied. Paquette and Bourke (1978b) have suggested that the driving force derives directly from local lateral pressure gradients causing shearing at the divergence or convergence of isopycnals. The general situation is illustrated schematically in Figure 18. Paquette and Bourke suggest that the direction of motion will not be directly down the pressure gradient, as shown, but will be more or less transverse, depending on the degree of geostrophic balance attained.

In an attempt to determine the source of forcing on a much larger scale, evidence will be presented in Section V which suggests an association between the upper level current direction, ice edge recession and the likelihood of fine-structure.

### 4. Finestructure Element Extent

The spatial and temporal extents of individual fine-structure elements have been deduced by a number of authors.

Through time-series measurements, Corse (1974) found a 6 hr duration and a 1 to 2 km spatial extent. Garrison et al. (1974) estimated a 0.6 to 1.3 km spatial extent and Zuberbuhler and Roeder (1976) found extents of 4 hr and 4 km. Paquette and Bourke (1978b) have suggested that much larger spatial extents may be found in the direction parallel to the ice edge.

The apparent short life of individual elements of finestructure is likely caused by their shape and their strong vertical temperature gradients. Once interleaving has taken place there is, within the water column, an element of water which has the appropriate density for its depth but an anomalously high temperature. This element has much more surface area in contact with the colder water around it than it had before interleaving and has strong temperature gradients. It will, therefore, lose heat much faster to the colder water around it than it would have if it had not interleaved. Unless it is being constantly supplied with heat its temperature gradients will be broken down and the element will decay. Gregg (1973) has suggested that gradients will be smoothed in time scales measured in minutes.

No time series were taken during the MIZPAC 77 cruise, but cross-section 7 was revisited after 3 days. Figure 14 shows this cross-section on 31 July 77 and Figure 15 shows the same cross-section on 2 August 77. Finestructure with the same general characteristics is found in the two figures but no individual elements appear to have survived

in place. This indicates that, although the finestructure elements in the earlier cross-section have either decayed or been carried away by the currents, they have been replaced by others. It would appear that the same general process which created the finestructure has been going on in the area for at least 3 days. The observation that elements are replaced by similar ones was also made by Zuberbuhler and Roeder (1976) upon analysis of stations revisited during the MIZPAC 75 cruise.

#### D. THE ALASKAN COASTAL CURRENT

Because of its importance in melting the ice along the coast to allow shipping, the Alaskan Coastal Current has been examined separately. Figures 19 through 24 are temperature and salinity cross-sections of the current looking downstream, progressing from west to east. The cross-section positions can be seen in Figure 2.

Figure 19 shows a wide, horizontally stratified current with a maximum temperature between  $9^{\circ}$  and  $10^{\circ}\text{C}$ . The water in this area has not yet been much cooled. The cold temperatures and high salinities near the bottom left of the figure show where the upper level currents have overridden the resident northern water.

In Figure 20, the overall current is still wide but its core has been narrowed significantly. Its maximum temperature is now between  $8^{\circ}$  and  $9^{\circ}\text{C}$ . Northern water is still evident in the lower left of the figure.

In Figure 21, the current has been narrowed still further and has moved closer to shore. The maximum temperature is still between  $8^{\circ}$  and  $9^{\circ}\text{C}$ . The bottom here is significantly deeper but the warm current has not deepened. Rather, the deeper waters have the characteristics of northern water.

By Figure 22, the current has squeezed up against the coast and shows the first evidence of submerging. It still has maximum temperatures greater than  $8^{\circ}\text{C}$ .

In Figure 23, the current is shown just to the west of Point Barrow. It is still squeezed up against the coast and has submerged. Its maximum temperature has been lowered to between  $7^{\circ}$  and  $8^{\circ}\text{C}$ .

Figure 24 is a cross-section due north of Point Barrow. It shows the current core submerged to about the same depth as in Figure 23 but with a maximum temperature now of less than  $7^{\circ}\text{C}$ .

The general pattern, wherein it narrows against the coast and is submerged off Point Barrow, agrees with the flow as shown by Paquette and Bourke (1974).

#### E. UPPER LEVEL CURRENTS

Paquette and Bourke (1978b) indicated that insolation falling directly on the southern fringes of the ice pack is only 0.1 to 0.2 as great as is necessary to account for the observed rate of recession of the ice edge. Hence, melting is concentrated at the line of contact of warm southerly water and the ice. As indicated in Section IV(B), in the southern area the currents in the upper layer are significantly

warmer and swifter than those in the lower layer. Consequently, it is the upper layer currents which are expected to carry most of the heat to the ice. Therefore, a coupling of the recession of the ice edge and the upper level currents is suggested. In those areas where the upper level currents are directed toward the ice, they will carry more heat to the ice and the ice edge will be expected to recede more quickly. This coupling was the basis for the following procedure to infer the directions of the upper level currents in the Chukchi Sea during the melt season of 1977.

Positions of the ice edge were taken from National Oceanographic and Atmospheric Administration (NOAA) ice analysis charts and were plotted in Figure 25. Three positions of the ice edge were depicted: 12-13 July, 19-20 July and 31 July to 3 August 77. Where there was significant movement of the ice edge, the currents were assumed to be toward the ice. Where there was little or no recession of the ice edge, the currents were assumed to be either essentially parallel to the ice edge or essentially stopped. Using these principles, it was found that the inferred flow conformed well with the pattern of Coachman et al. (1975, page 142). The vectors shown in Figure 25 are the result of altering their vectors slightly to conform to the ice edge recession of 1977. Other circulation patterns by the U. S. Navy Hydrographic Office, HO 705 (1958) and Potocsky (1975) were found to be in somewhat poorer agreement.

Probably the most obvious difference between the upper level current directions suggested by the ice edge movements

of 1977 and those indicated by Coachman et al. (1975) is the gyre off Point Barrow. This gyre does appear in Potocsky and Ho 705. Also, it has been noticed in the movement of the ice in time lapse photographs taken from a camera mounted on a platform at Point Barrow (M. A. Beal, Pers. Comm.) and in the drift of ice camps in MIZPAC 71 (Garrison and Pence, 1973). Added evidence for the gyre may be seen in the dynamic topographies shown in Figures 26 and 27. These are plots of the surface dynamic heights referenced to 40 m. It is well known that the baroclinic component of the flow in the Chukchi Sea is only a fraction of the total. Therefore, one may suspect that the 10 to 14 cm/sec of baroclinic velocity deduced from these diagrams is accompanied by a similar, but larger, barotropic flow.

Figure 26 is not synoptic, but it still shows a dynamic depression off Point Barrow at the position indicated as Point C. Figure 27 shows the surface dynamic heights for cross-sections 6 and 7B which were perpendicular to each other and were measured over a period of 20 hours. Figure 27 clearly shows a dynamic depression around Point C. This depression is consistent with the dynamic feature to be expected in the middle of a cyclonic gyre which is externally forced. The forcing for the establishment of the gyre is most likely lateral friction between the north-easterly flowing Alaskan Coastal Current and the northwesterly flowing Beaufort Gyre. These flows converge approximately perpendicularly off Point Barrow.

Although the core of the Alaskan Coastal Current turns right around Point Barrow (Paquette and Bourke, 1974), some of its heat is carried into the gyre. As was indicated in Section IV(D), the Coastal Current core was submerged by the time it reached Point Barrow. It can be seen in Figure 23 that the heat carried by the current was even evident below 60 m. Therefore, some of the heat carried into the gyre is deep and probably contributes to the formation of the deep finestructure found in the ice bay. In Section IV(C), it was shown that finestructure was as deep as 50 m in the bay.

Since there is no other heat source available to the gyre, especially at deeper depths, it must come from the Coastal Current. However, a study of the MIZPAC 77 temperature profiles has shown no continuous path for the heat. Therefore, it is probably supplied irregularly to the gyre, e.g., in pulses or surges. There is no direct evidence of this irregularity. However, the gyre does flow over the Barrow Canyon and flow reversals have been noted there (Mountain, 1976).

## V. DISCUSSION

Assuming that the upper level currents in Figure 25 are correct, the next step is to examine how they affect the likelihood of the presence of temperature fronts and temperature finestructure. To this end, data from each of the MIZPAC cruises have been considered and the following hypotheses have been formulated:

1. Where the upper level currents are parallel to the ice edge or are essentially stopped, little heat is transferred to the colder water and the ice edge does not recede quickly. There is little finestructure, but there may be temperature fronts.
2. Where upper level currents have a strong component normal to the ice, the ice edge recedes more quickly and there is more finestructure. Although temperature fronts are present in this area, they are harder to recognize. The temperature fronts in the upper layer are strongly tilted and terminate in a shallow zone of low salinity where the ice is melting rapidly. The front in the lower layer is diffuse and complicated with finestructure.

The following several sections show in some detail the cases in which the above hypotheses seem to be sustained.

### A. MIZPAC 77

#### 1. Point A

Point A in Figures 2, 25 and 26 is at  $70^{\circ}\text{N}$  and  $168^{\circ}\text{W}$ . The area in the vicinity of Point A is an example of a location where there is a sharp front, a lack of finestructure, slow ice edge recession and currents which do not have a strong component of velocity normal to the ice.

The currents flowing north bifurcate to the south of Point A creating a rather quiescent area in the vicinity of Point A. The effect of this current pattern on the ice edge melt-back is to produce a tongue of ice at Point A which protrudes southward. For approximately two weeks in 1977, the ice edge was relatively stationary and the warm currents flowed east or west near Point A instead of through it. This created a velocity shear between the northern water and the warm currents from the south which led to the formation of a strong vertical temperature front. It is in the area of Point A that temperature fronts, extending from the surface to the sea floor were found in 1975 and 1977. It is also an area where no finestructure was found during the MIZPAC 77 cruise. Finestructure was found in 1975 and will be discussed in Section V(E).

## 2. Point B

Point B in Figures 2, 25 and 26 is at  $71^{\circ}\text{N}$  and  $162^{\circ}\text{W}$ . The area in the vicinity of Point B is another example of a location where temperature fronts are coincident with a slow recession of the ice edge and with currents which do not have a strong component of velocity normal to the ice edge.

The upper level currents here appear once more to bifurcate while the ice edge has receded only slightly more

than at Point A. Therefore, the situation from the surface to a depth of approximately 20 m is much the same as at Point A and temperature fronts are once more found. These fronts were shown in Figures 6 to 9. The water above the thermocline is warm Alaskan Coastal Current water which has not mixed with the cold northern water below. A sharp, nearly horizontal thermocline is formed. Thus, there is little or no finestructure in this region. Finestructure, however, may be present some distance to the south where the relatively warm lower layer from the south comes in contact with the cold northern water. As discussed earlier, Point B is in an area where the upper and lower layer currents appear to be completely uncoupled.

### 3. Point C

Point C is at  $71^{\circ}35'N$  and  $158^{\circ}W$ . It is in the middle of the cyclonic gyre off Point Barrow. The area in the vicinity of Point C is an example of a location which is very different from Points A and B. Here the currents do have a strong component toward the ice, the ice recedes relatively quickly and there is extensive finestructure.

Since the upper level currents turn toward the ice as they pass Point Barrow, the ice edge recedes more quickly here than at adjacent positions. This causes the bay to be formed. At the time of the MIZPAC 77 cruise, the melting of the ice in the bay was virtually complete, but the northern water below it was still in the process of interleaving with modified Alaskan Coastal Current water. This was indicated by the frequent presence of finestructure in the area around

Point C. The presence of the deep structure was possible because the Alaskan Coastal Current was deep when it supplied heat to the gyre.

B. MIZPAC 71

In Figure 28, the upper level currents from Figure 25 were superimposed on a chart of the ice edge position and finestructure distribution for the MIZPAC 71 cruise. In so doing, the assumption has been made that the currents in the area represented by Figure 28 were the same in 1971 as in 1977. Although this consistency has not been conclusively proved, it will be shown in the forthcoming figures that the current directions from Figure 25 do, in fact, fit well with the shape of the ice edge for each MIZPAC year except 1975. As will be discussed in Section V(E), 1975 was an anomalous year in other ways as well.

In the area represented by Figure 28, the assumed currents were generally parallel to the ice edge except in the gyre off Point Barrow. Also, all of the finestructure indicated in Figure 28 is within this gyre. It is difficult to draw any general conclusion from Figure 28 alone, but it can be observed that areas where currents are parallel to the ice edge coincide with areas lacking finestructure, just as they did in 1977.

C. MIZPAC 72

In Figure 29, the upper level currents from Figure 25 were superimposed on a chart of the ice edge and finestructure

distribution from MIZPAC 72. As noted in the previous section, the shape of the ice edge seems to be consistent with these currents. Figure 29 also includes the isotherms of the maximum temperature in the water column.

At the time of the MIZPAC 72 cruise, the ice had melted back more than during any of the other cruises. As evidenced by the isotherms in Figure 29, the areas where the largest amount of finestructure was usually found was warmer than in the other years and finestructure was not present to a great extent. However, the area in the gyre off Point Barrow still had remnants of weak finestructure where there was ice left. The only area where strong finestructure is indicated is in the left of Figure 29. It will be noted that it exists 125 km south of the ice at one point and 35 km behind the ice edge in another, occurrences not readily explainable with the existing data. Although finestructure far from the ice edge has not been found often, it may simply be a result of most stations having been occupied close to the ice edge.

#### D. MIZPAC 74

In Figure 30, the upper level currents from Figure 25 were superimposed on a chart of the ice edge positions and the finestructure distribution from the MIZPAC 74 cruise. Once again, the currents fit well with the shape of the ice edge. As this was the earliest of the MIZPAC cruises, the ice had not melted back as far as it had during the other cruises. The assumed current pattern is seen to cross the ice edge in a great many places. Consequently, there are large areas

where finestructure is present, especially where the currents cross the ice edge nearly orthogonally. Again there is some finestructure 100 km or more south of the ice, indicating that water mass interleavings are not necessarily confined to the immediate vicinity of the ice.

#### E. MIZPAC 75

Analysis of the MIZPAC 75 data by Zuberbuhler and Roeder (1976) pointed out two things that made that year anomalous. The Alaskan Coastal Current was found to be farther seaward than in previous years and substantial areas of strong to moderate finestructure were found mainly in the gyre off Cape Lisburne, much farther from the ice edge than usual. Because the Coastal Current was farther seaward, the current directions from Figure 25 could not be transferred directly to the ice edge chart for 1975. Instead, in Figure 31 they were adjusted to seaward, north of Cape Lisburne, to a distance that fit well with the shape of the isotherms of maximum temperature in the water column. The gyre off Cape Lisburne was then expanded to fill the area from the coast to the new current arrows. Once this was done, the strongest finestructure was once again found in areas where the currents crossed the ice edge orthogonally.

Two explanations now appear for the presence of the finestructure in the region of the gyre off Cape Lisburne. One possibility is that the finestructure was formed by the interleaving of the water in the gyre with the currents flowing past Cape Lisburne. The second possibility is that the

finestructure was formed in the northern part of the gyre and was then carried by the currents in the gyre to the position where it was found.

## VI. CONCLUSIONS

Data gathered during the MIZPAC 77 cruise to the Chukchi Sea were displayed and analyzed with special attention being paid to finestructure and fronts. The phenomena observed in 1977 were compared with those seen in previous cruises and the following conclusions resulted:

- Upper level currents in the Chukchi Sea were inferred from the ice edge recession rates from 12 July to 3 August 1977 and from ice edge shapes for previous MIZPAC cruises. The current patterns were found to be in general agreement with those previously published, but are more detailed and are considered to be somewhat more valid.
- It was found that during the melt season in the Chukchi Sea finestructure has a geographical distribution which is coupled with the direction of the warm upper level currents. Where the currents had a strong component toward the ice, there was extensive finestructure. Where the component toward the ice was weak, there was little or no finestructure.
- Sharp vertical temperature fronts were observed at the ice edge in areas where inferred upper level currents bifurcated and created an area of slow ice recession. In one area, the front extended from the surface to the sea floor. In another area, where the warm upper level

currents had overridden colder resident water, the fronts were only from the surface to approximately 20 m depth.

- Six cross-sections of the Alaskan Coastal Current were displayed. The current was initially wide with its warmth at the surface. It narrowed considerably at the head of Barrow Canyon and was pressed against the coast. By the time it reached Point Barrow, the current had submerged and its warmth could be detected as deep as 60 m.
- Off Point Barrow a peculiar ice bay was discovered which had been observed in MIZPAC 71 and 72 but had not been well documented. The area of this bay was found to be a region of intense finestructure activity.
- In the ice bay off Point Barrow, finestructure was found deeper in MIZPAC 77 than in any of the previous years. It was postulated that the heat for this structure was supplied from the Alaskan Coastal Current after its warm core had submerged off Point Barrow.

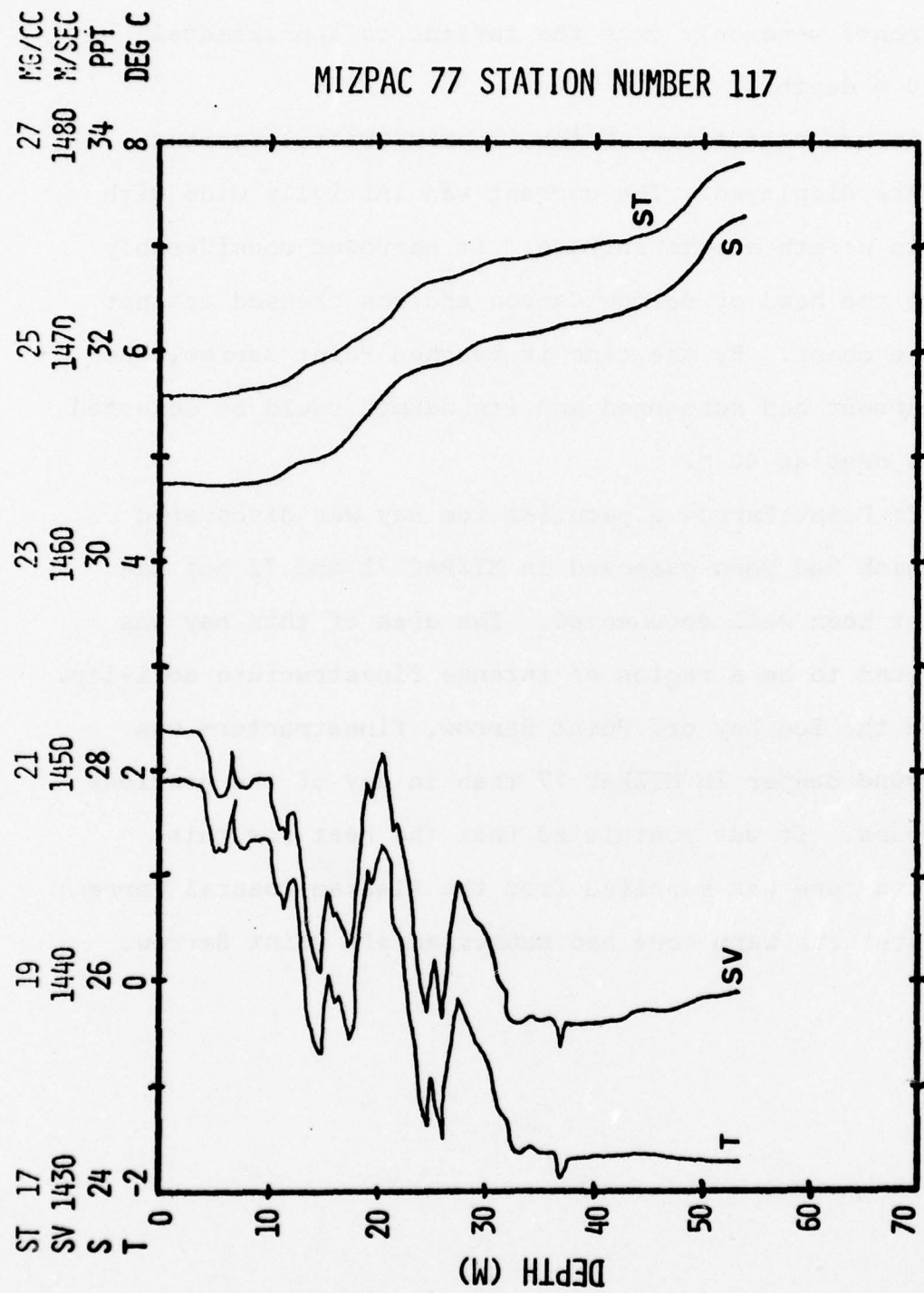


Figure 1. Property profiles for a station showing strong finestructure.

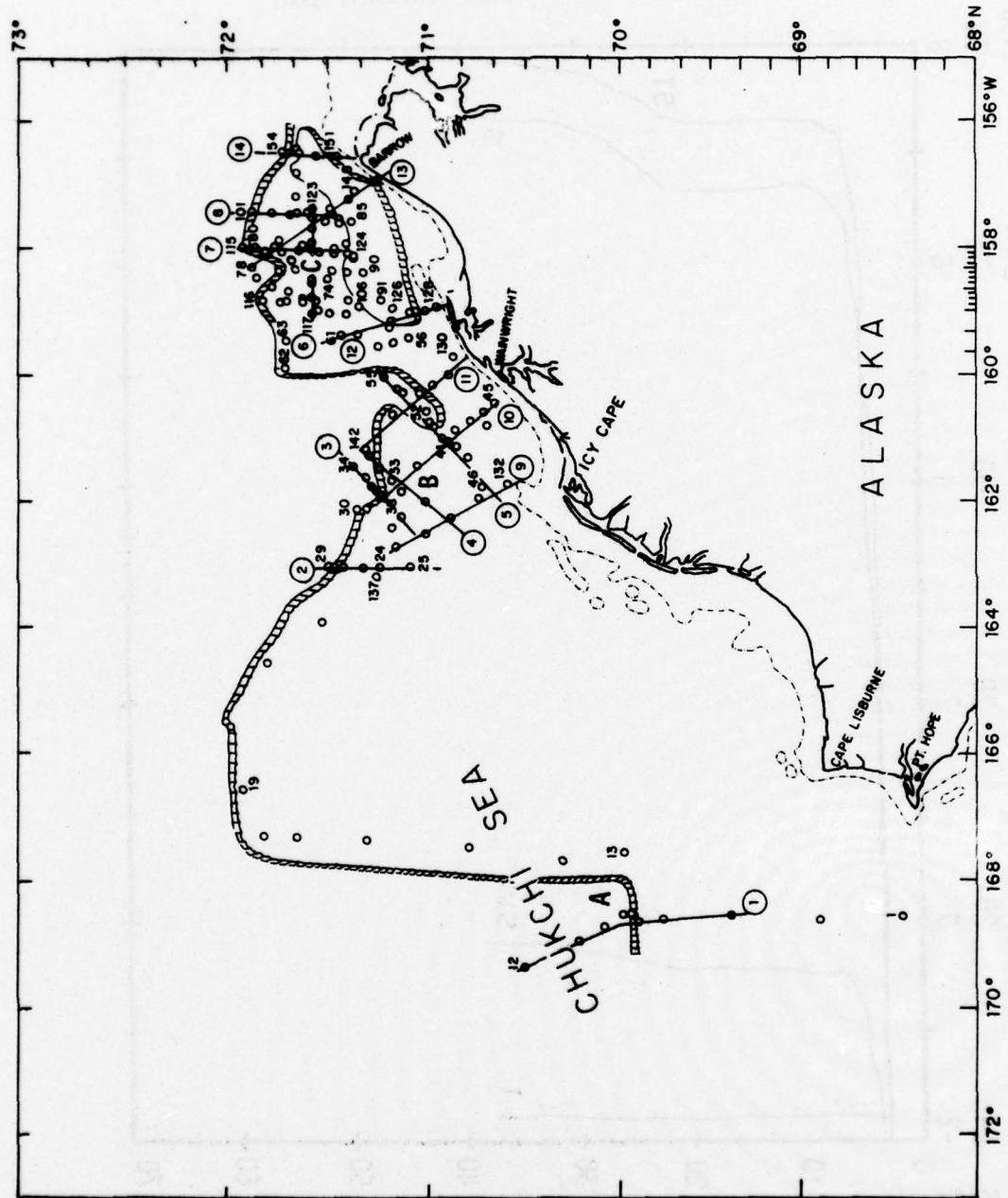


Figure 2. MIZPAC 77 station plot. The position of the ice edge at the time of observation is also shown (after Paquette and Bourke, 1978a). The bold straight lines indicate positions of temperature-salinity cross-sections.

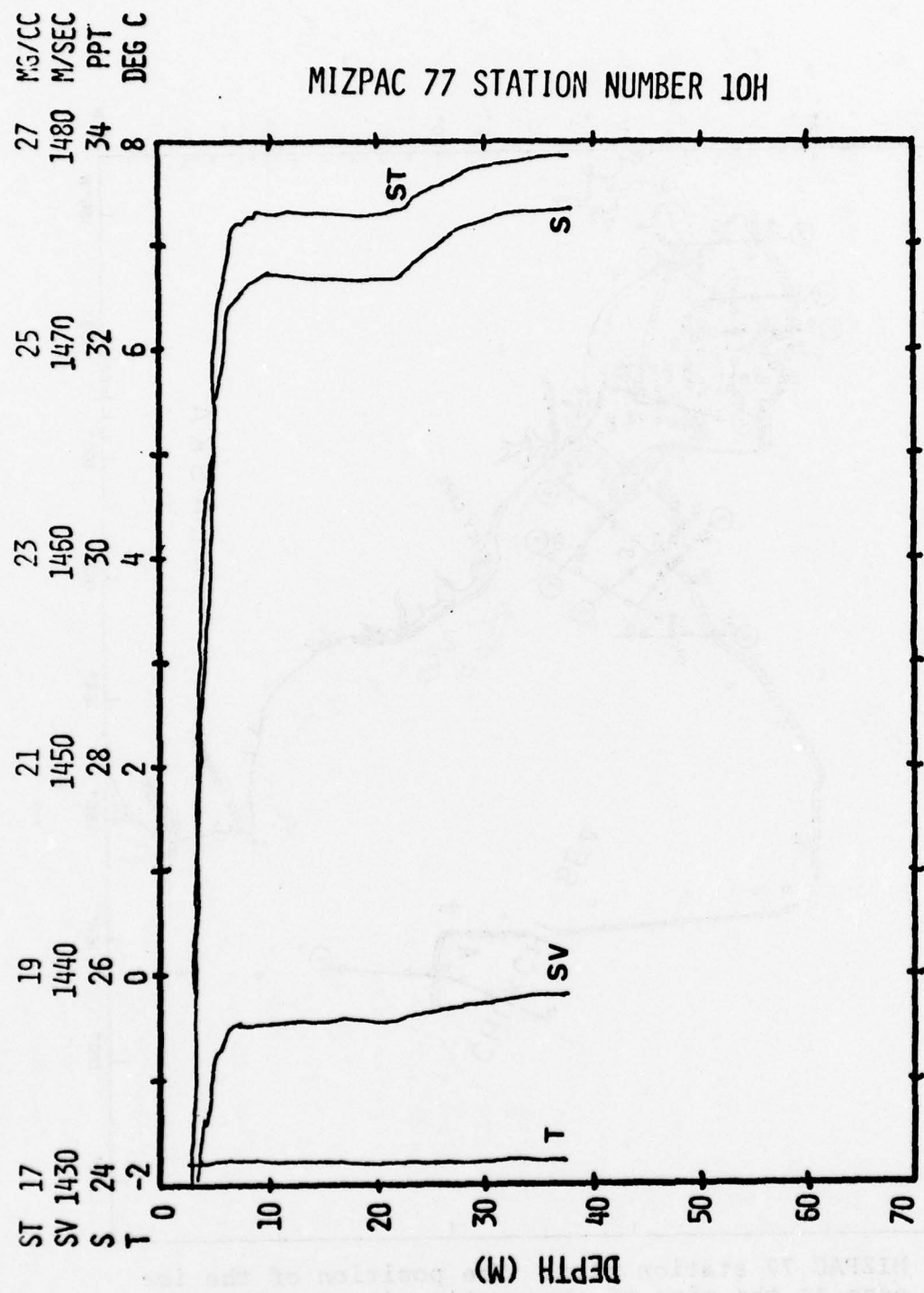


Figure 3. Property profiles of a representative station in the northern area.

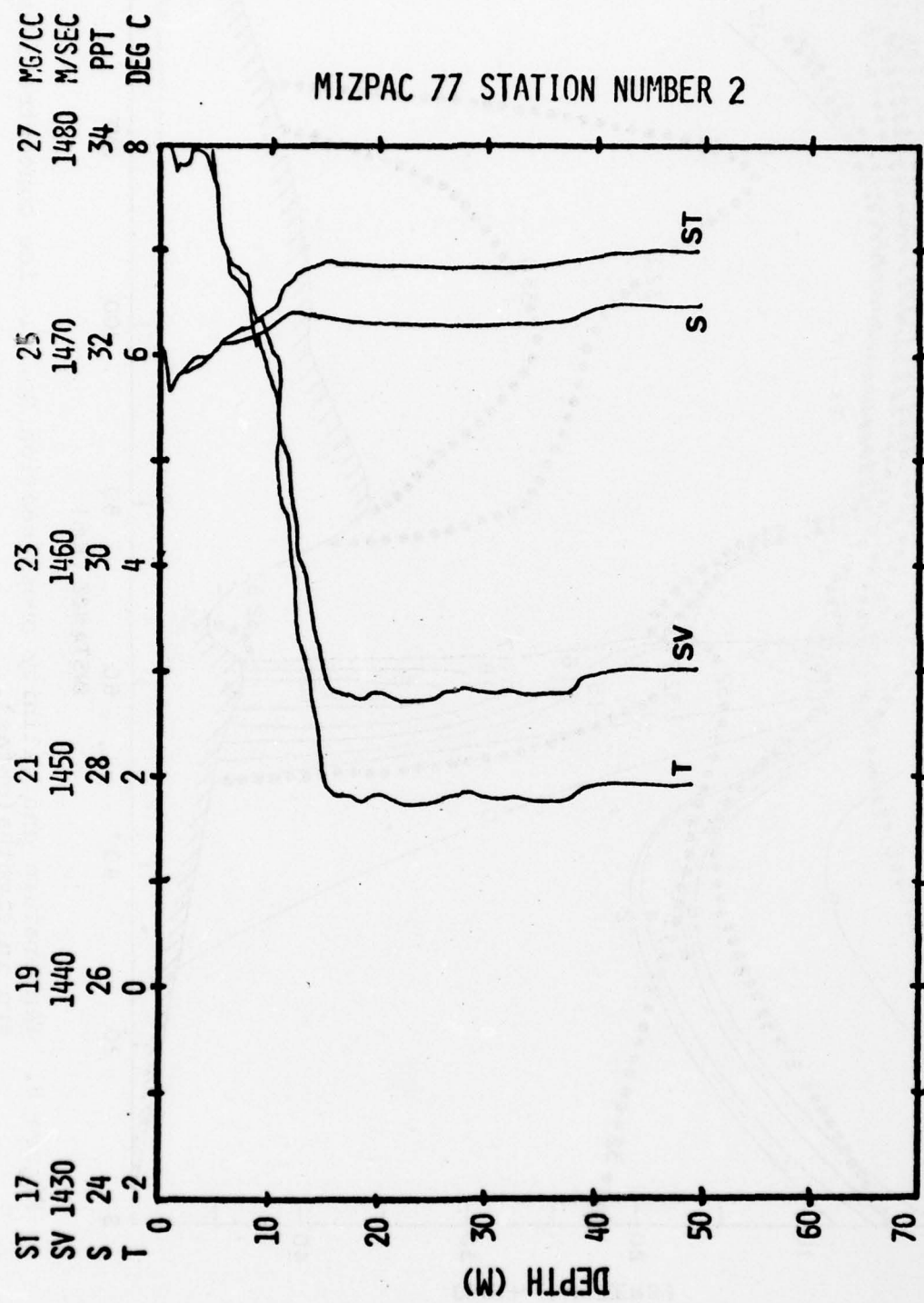


Figure 4. Property profiles of a representative station in the southern area.

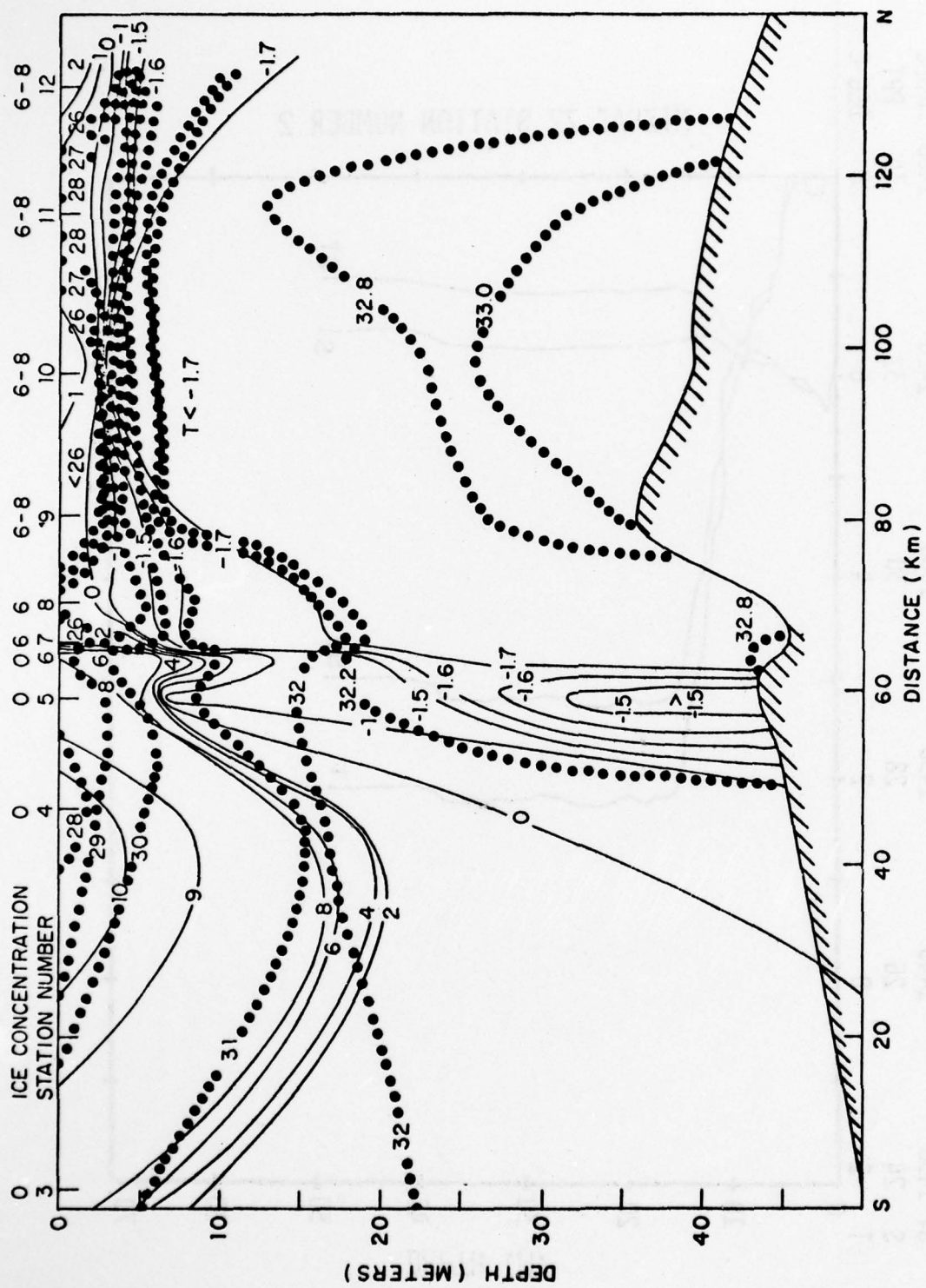


Figure 5. Temperature and salinity cross-section No. 1. Ice concentrations are in eighths (oktas).

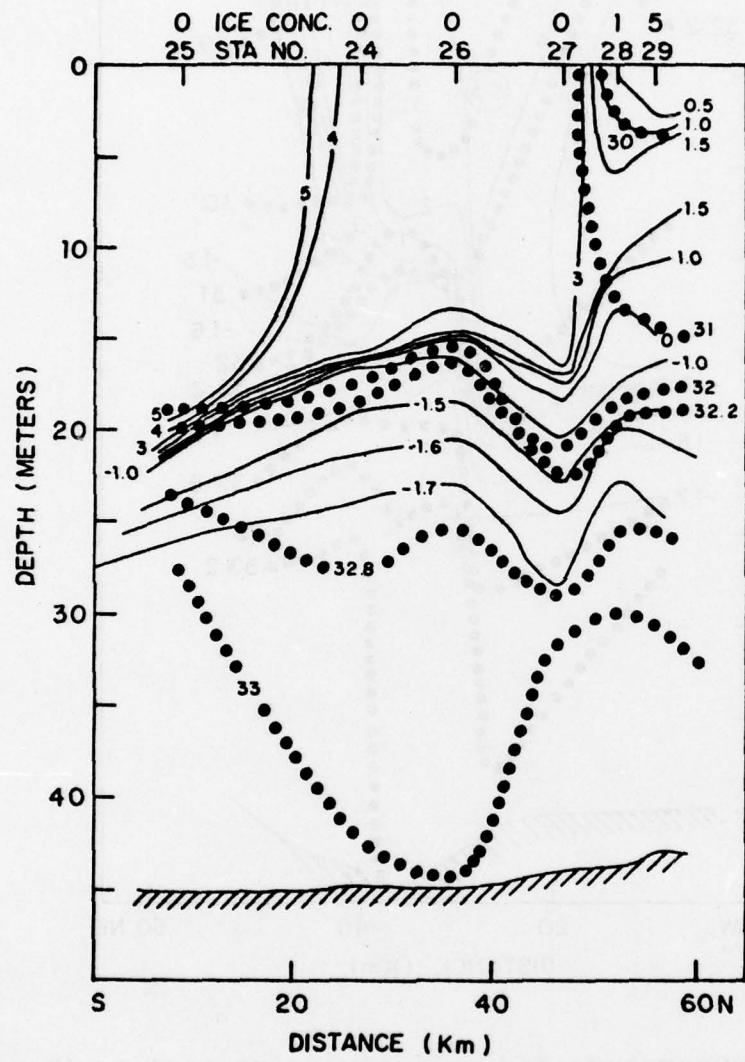


Figure 6. Temperature and salinity cross-section No. 2.  
Ice concentrations are in eighths(oktas).

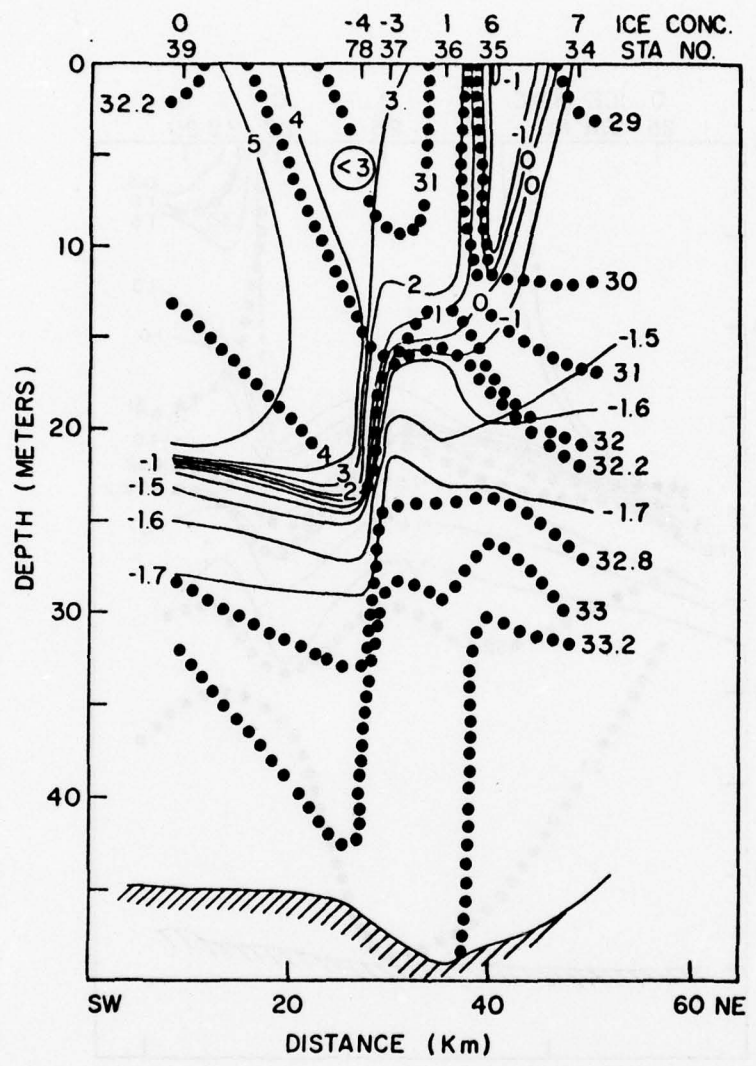


Figure 7. Temperature and salinity cross-section No. 3. Ice concentrations are in eighths(oktas) except that a negative value,  $-b$ , indicates a concentration of  $10^{-b}$ .

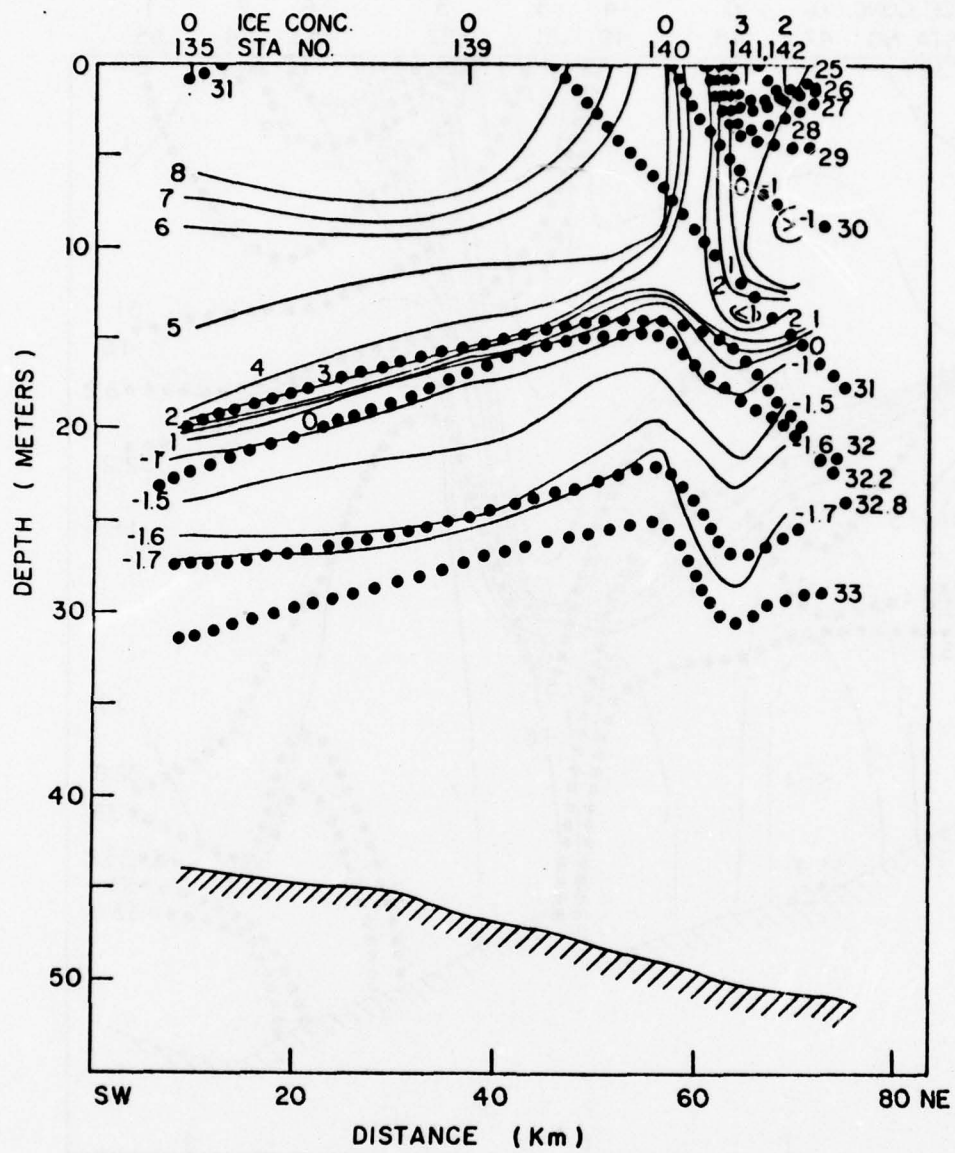


Figure 8. Temperature and salinity cross-section No. 4.  
Ice concentrations are in eighths(oktas).

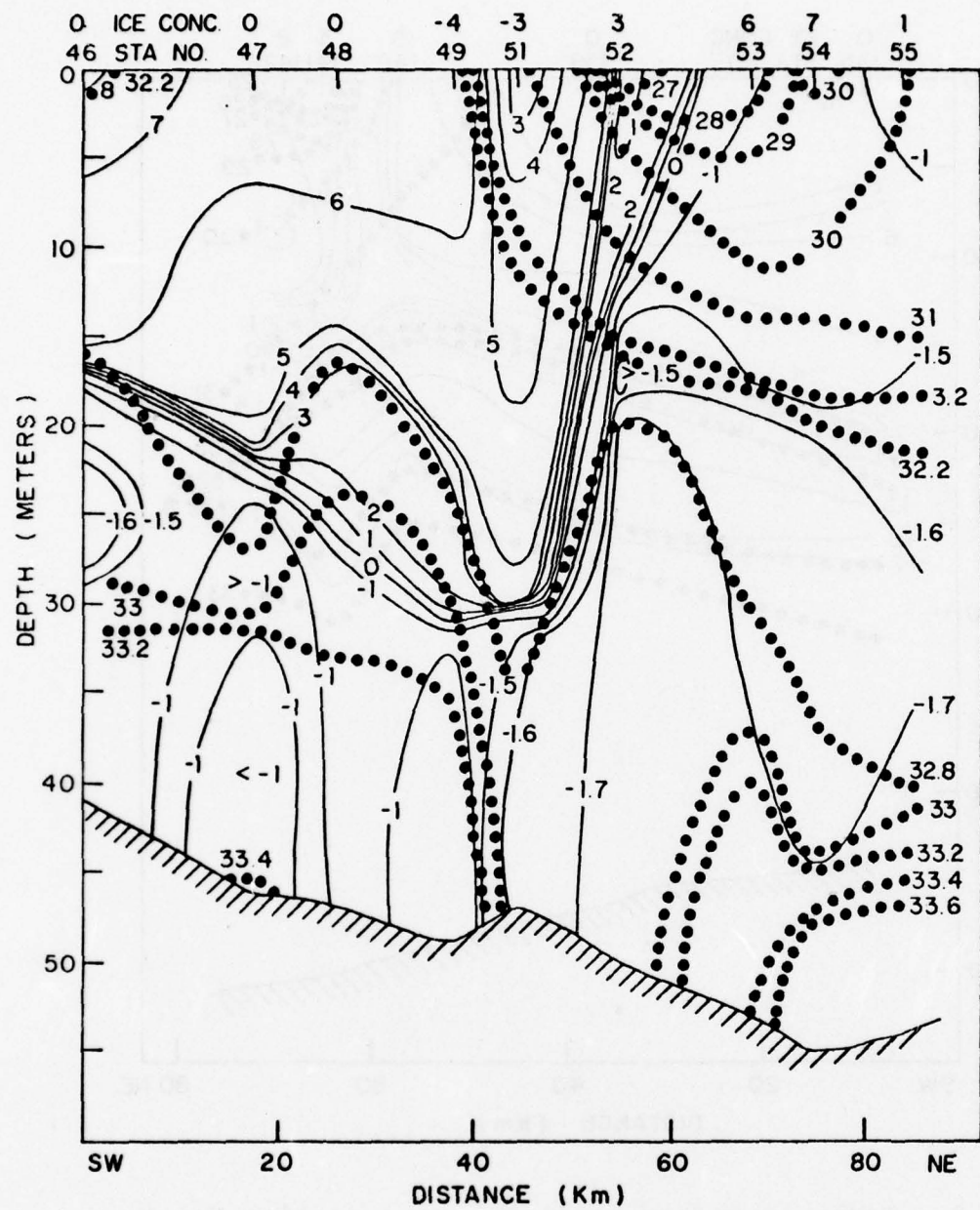


Figure 9. Temperature and salinity cross-section No. 5. Ice concentrations are in eighths(oktas) except that a negative value,  $-b$ , indicates a concentration of  $10^{-b}$ .

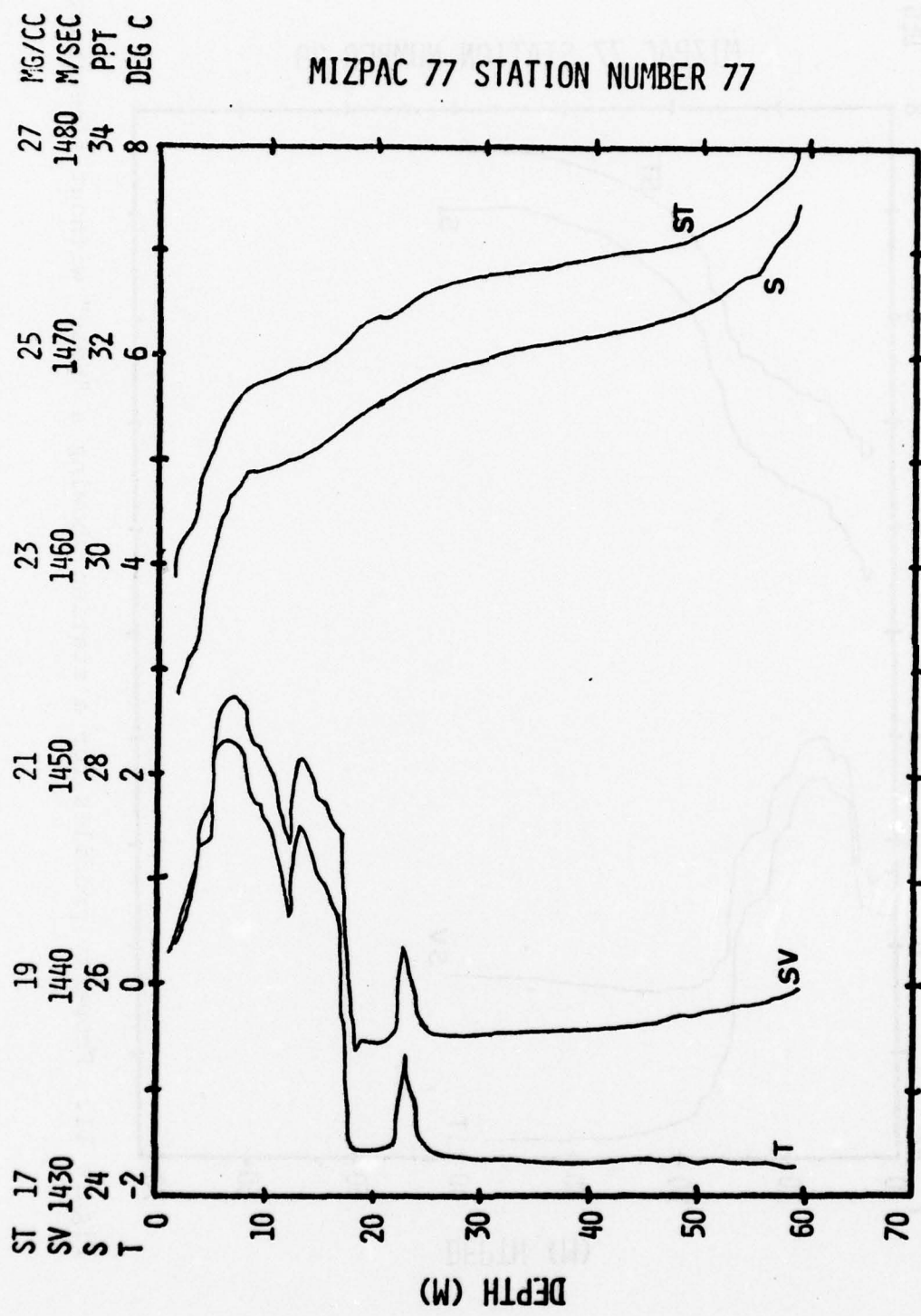


Figure 10. Property profiles for a station showing a "nose" with finestructure.

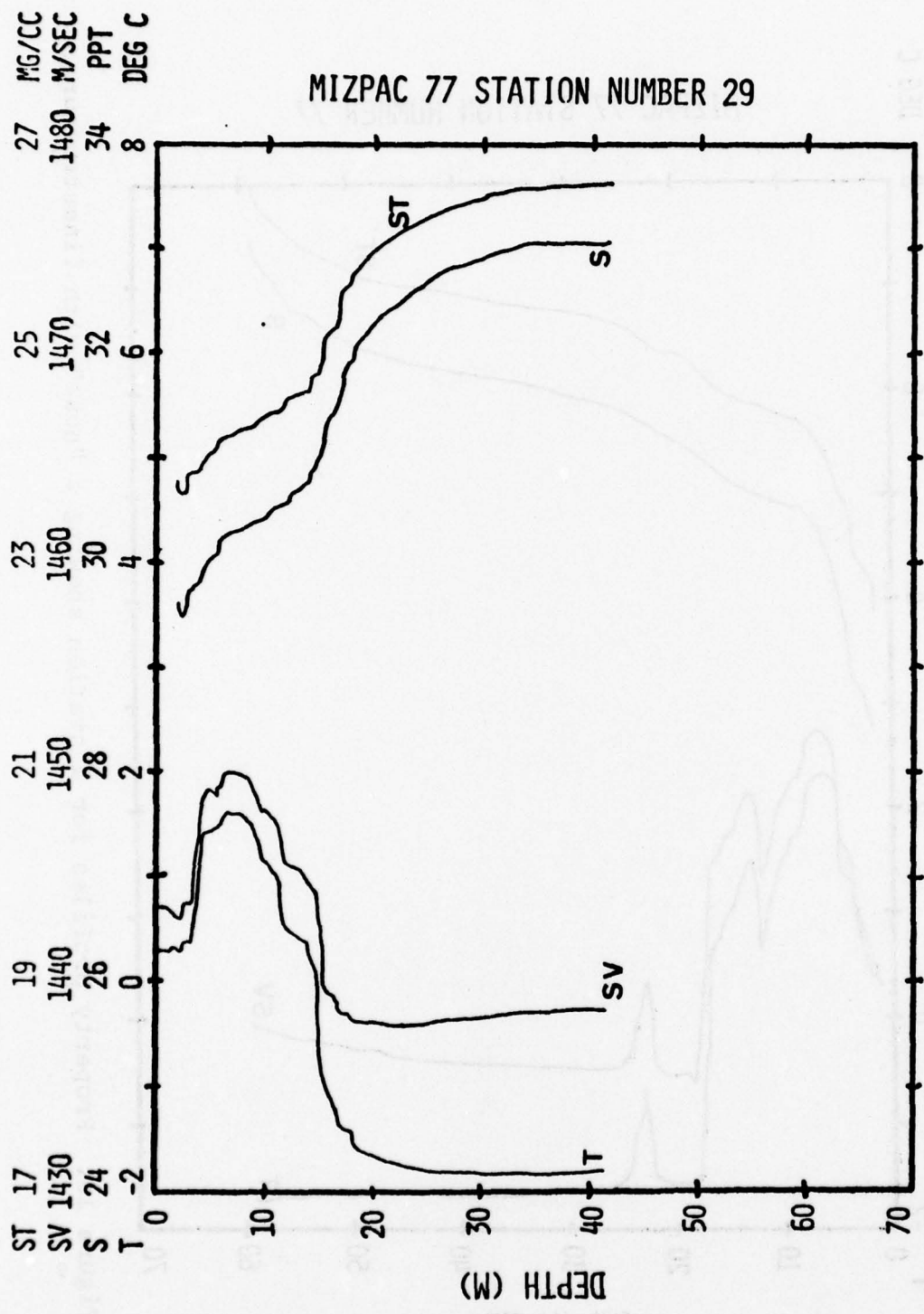


Figure 11. Property profiles for a station showing a "nose" without finestructure.

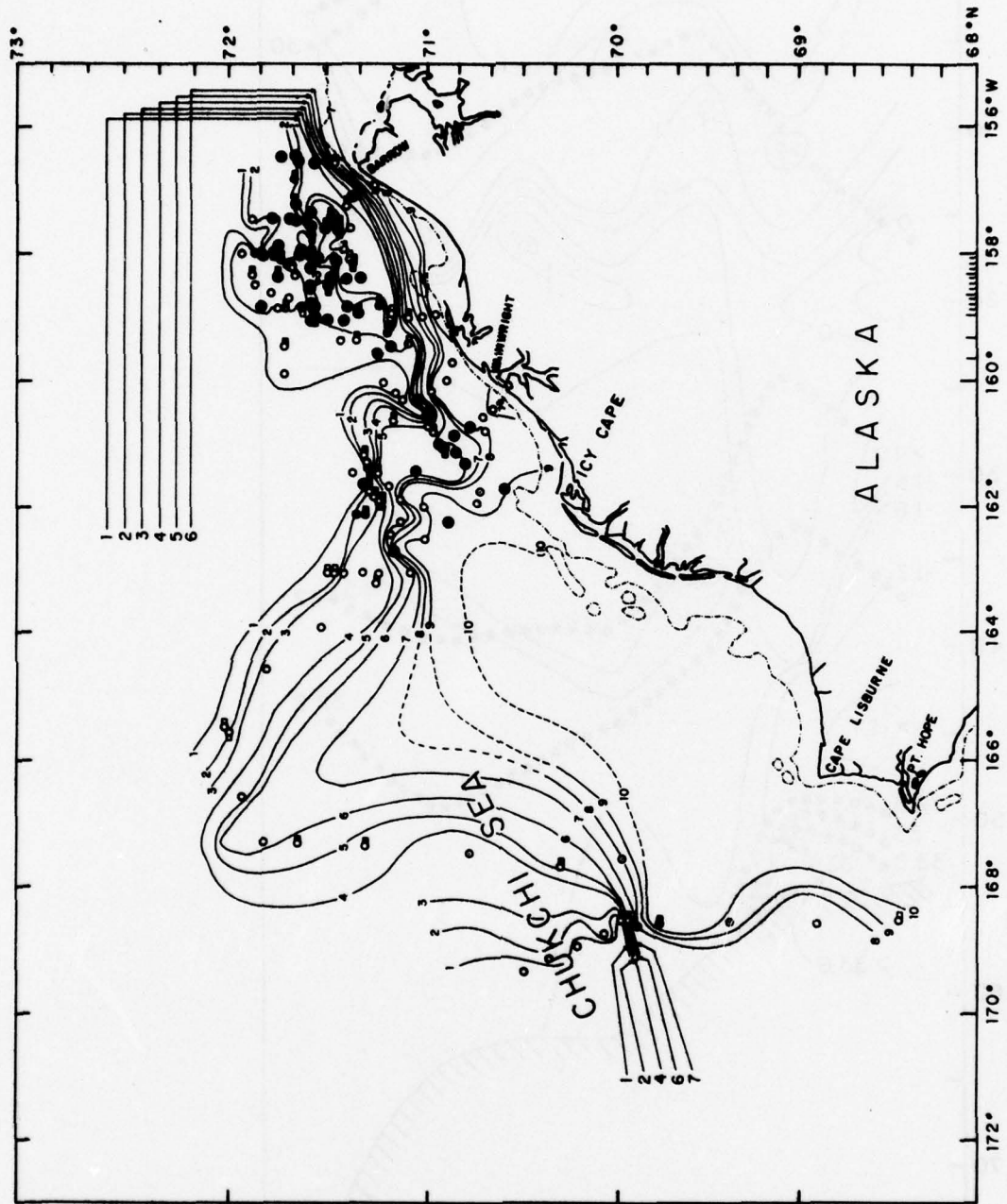


Figure 12. Distribution and intensity of fine structure during MIZPAC 77 (after Paquette and Bourke, 1978a). Symbols are described in Table II. Isotherms are the maximum temperature in the water column.

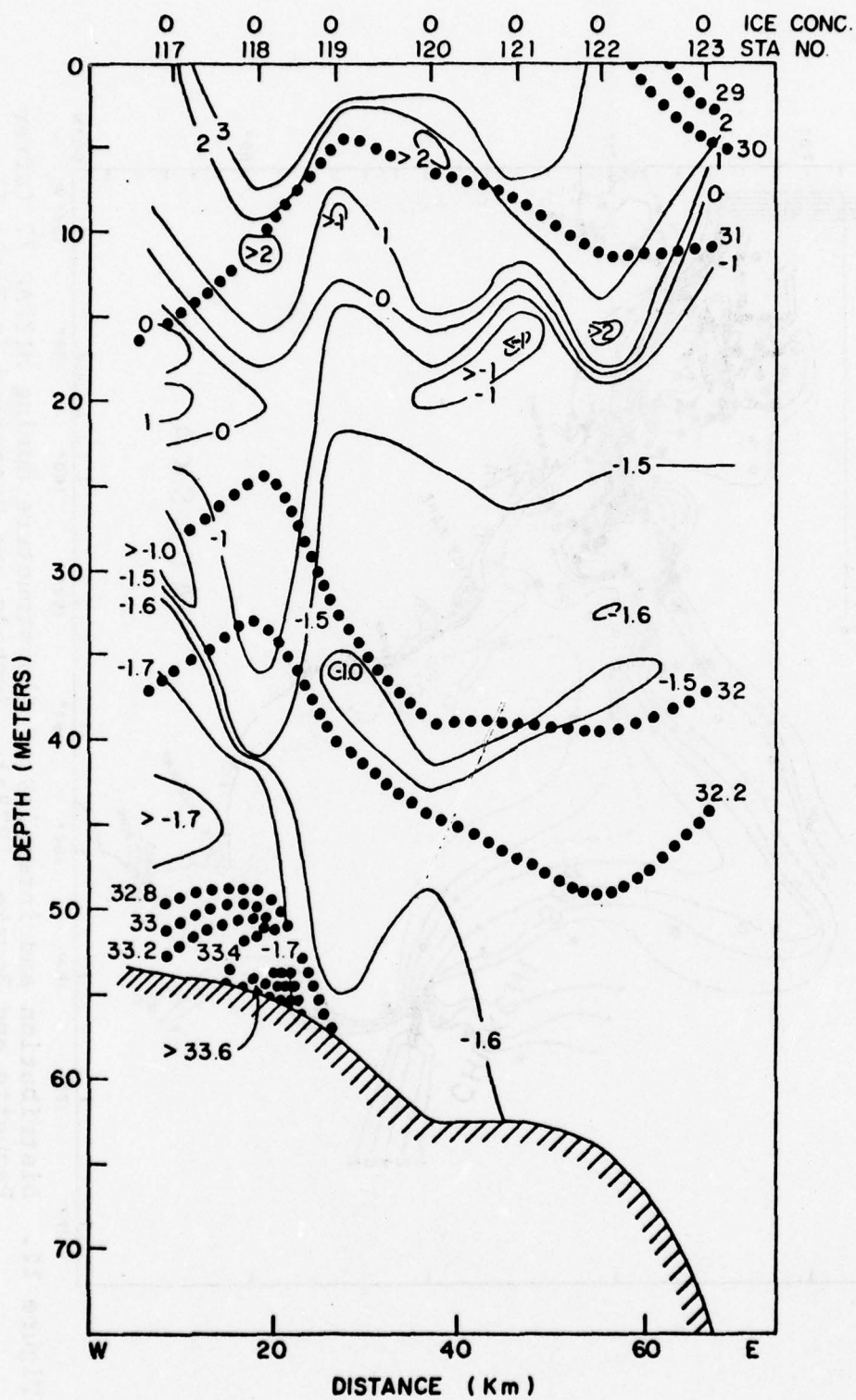


Figure 13. Temperature and salinity cross-section No. 6.  
Ice concentrations are in eighths (oktas).

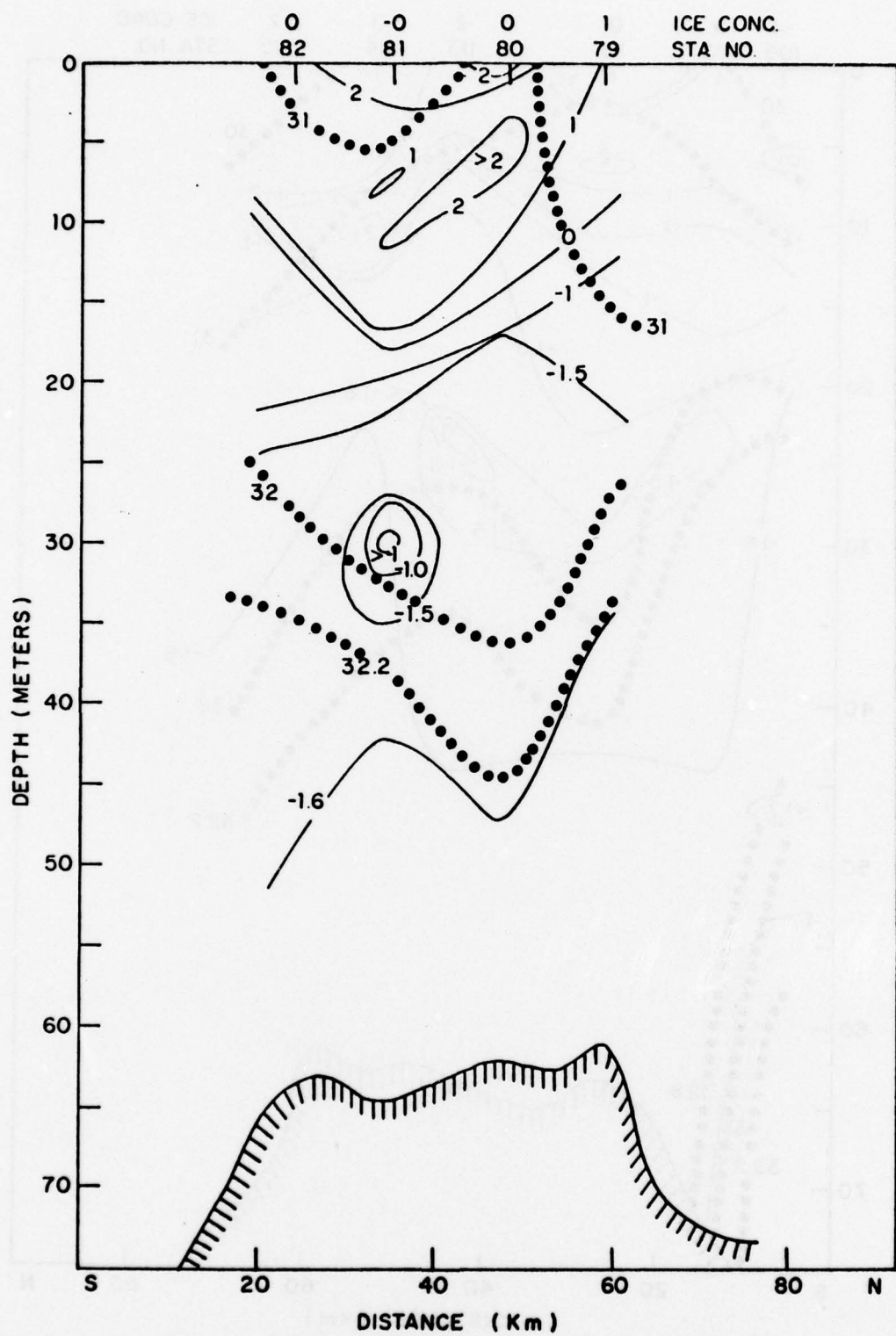


Figure 14. Temperature and salinity cross-section No. 7A. Ice concentrations are in eighths (oktas) except that a negative value,  $-b$ , indicates a concentration of  $10^{-b}$ .

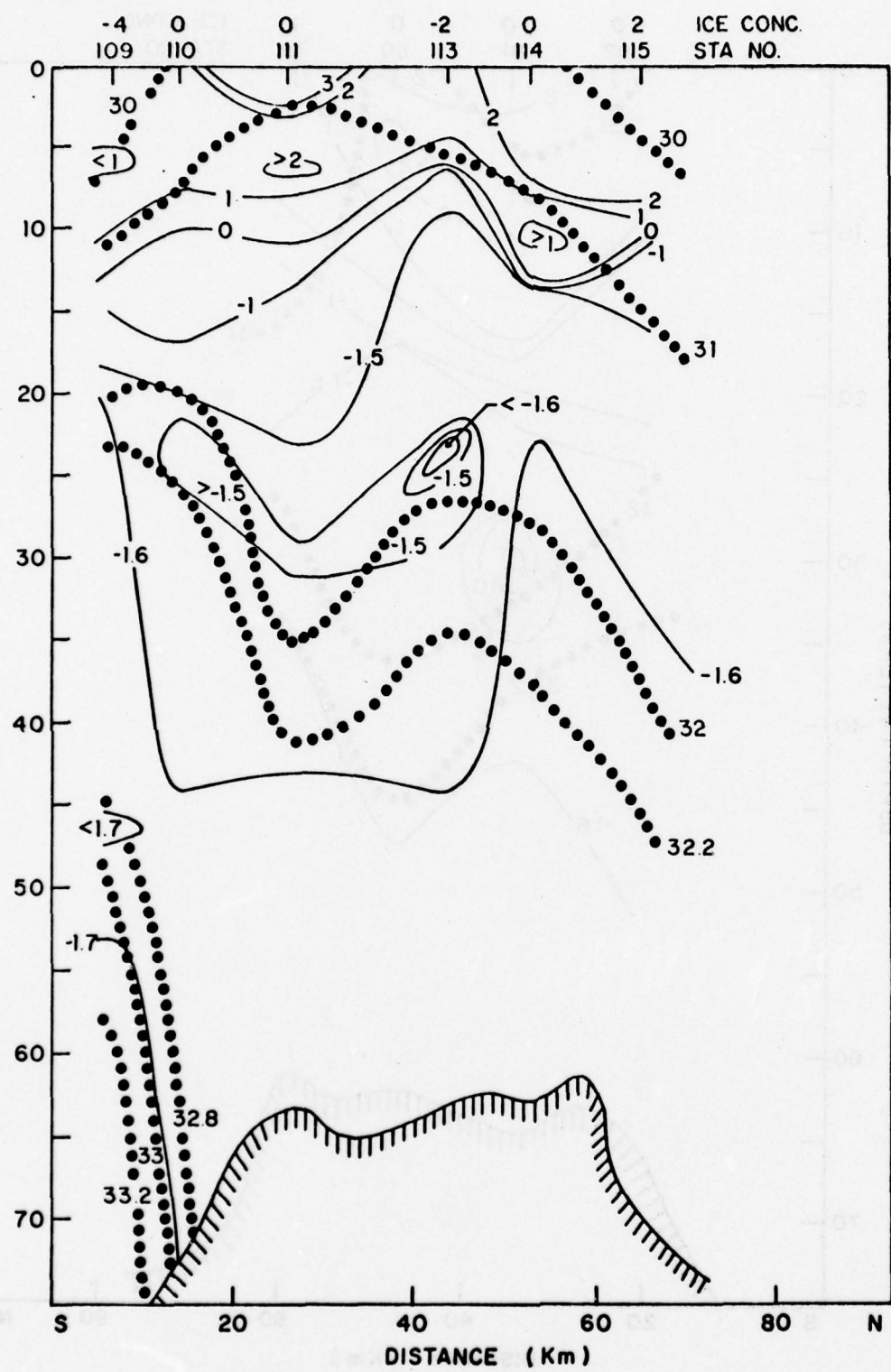


Figure 15. Temperature and salinity cross-section No. 7B. Ice concentrations are in eighths(oktas) except that a negative value,  $-b$ , indicates a concentration of  $10^{-b}$ .

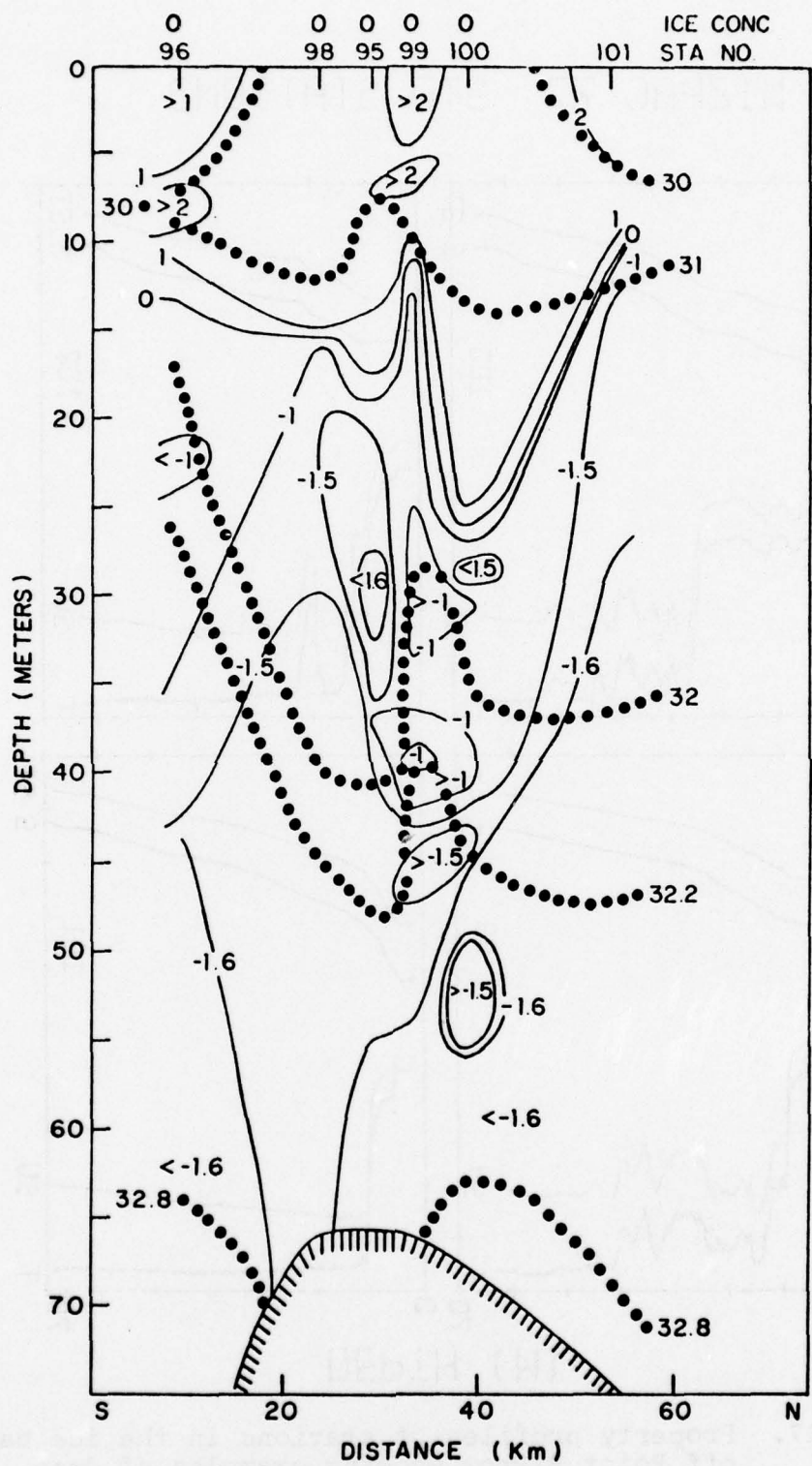


Figure 16. Temperature and salinity cross-section No. 8.  
Ice concentrations are in eighths (oktas).

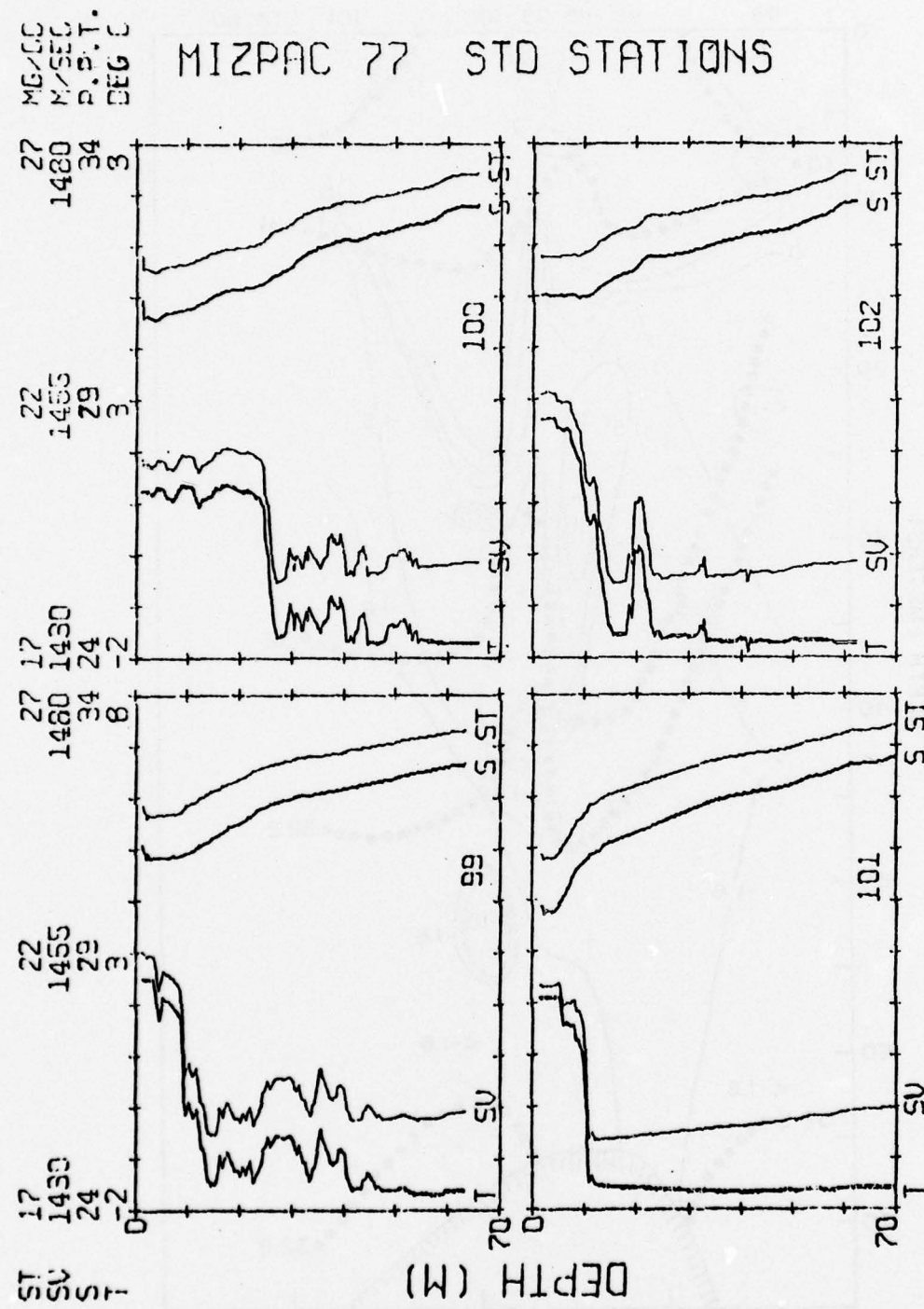


Figure 17. Property profiles of stations in the ice bay off Point Barrow showing examples of deep finestructure.

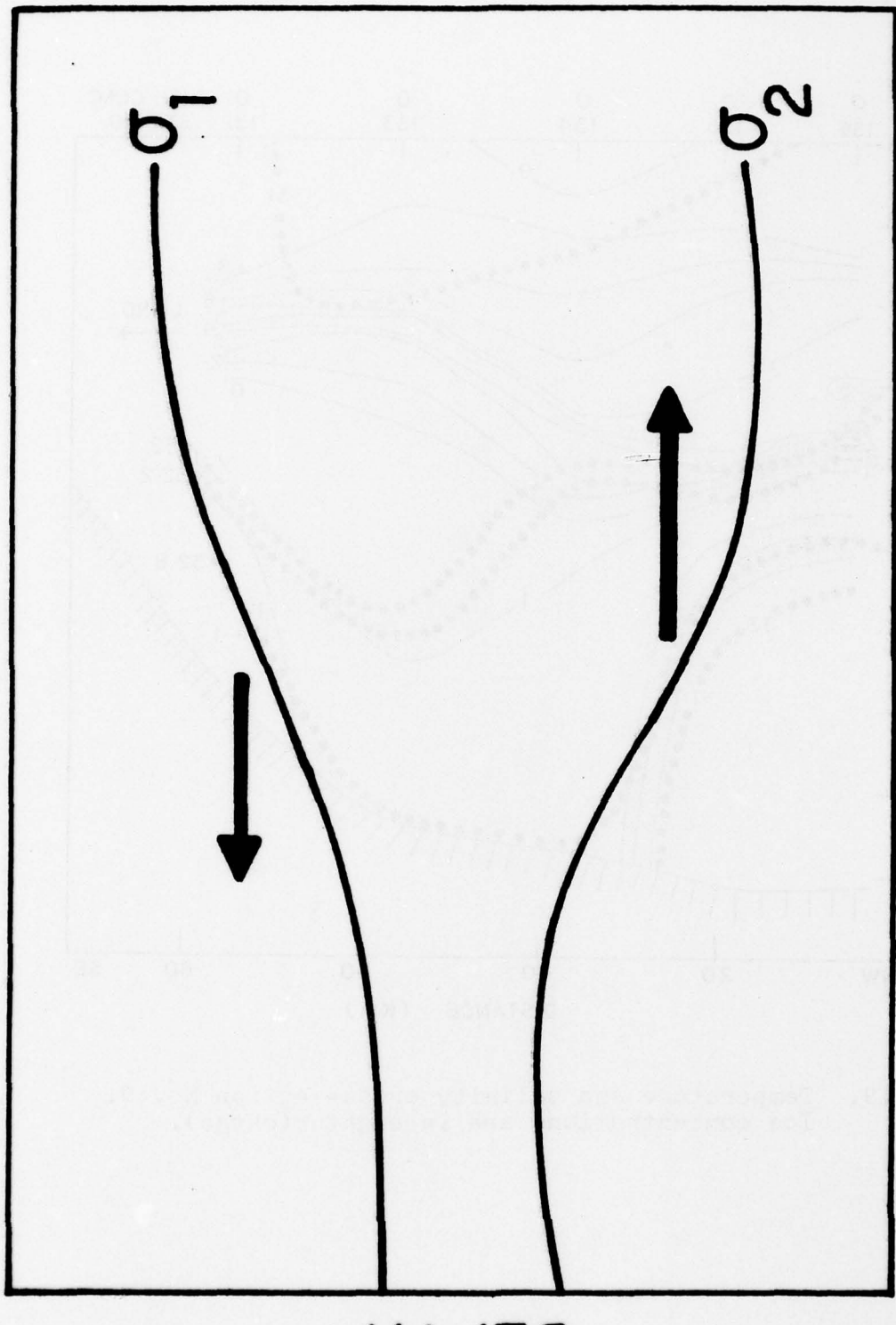


Figure 18. Schematic of a portion of a vertical density cross-section (after Paquette and Bourke, 1978b).

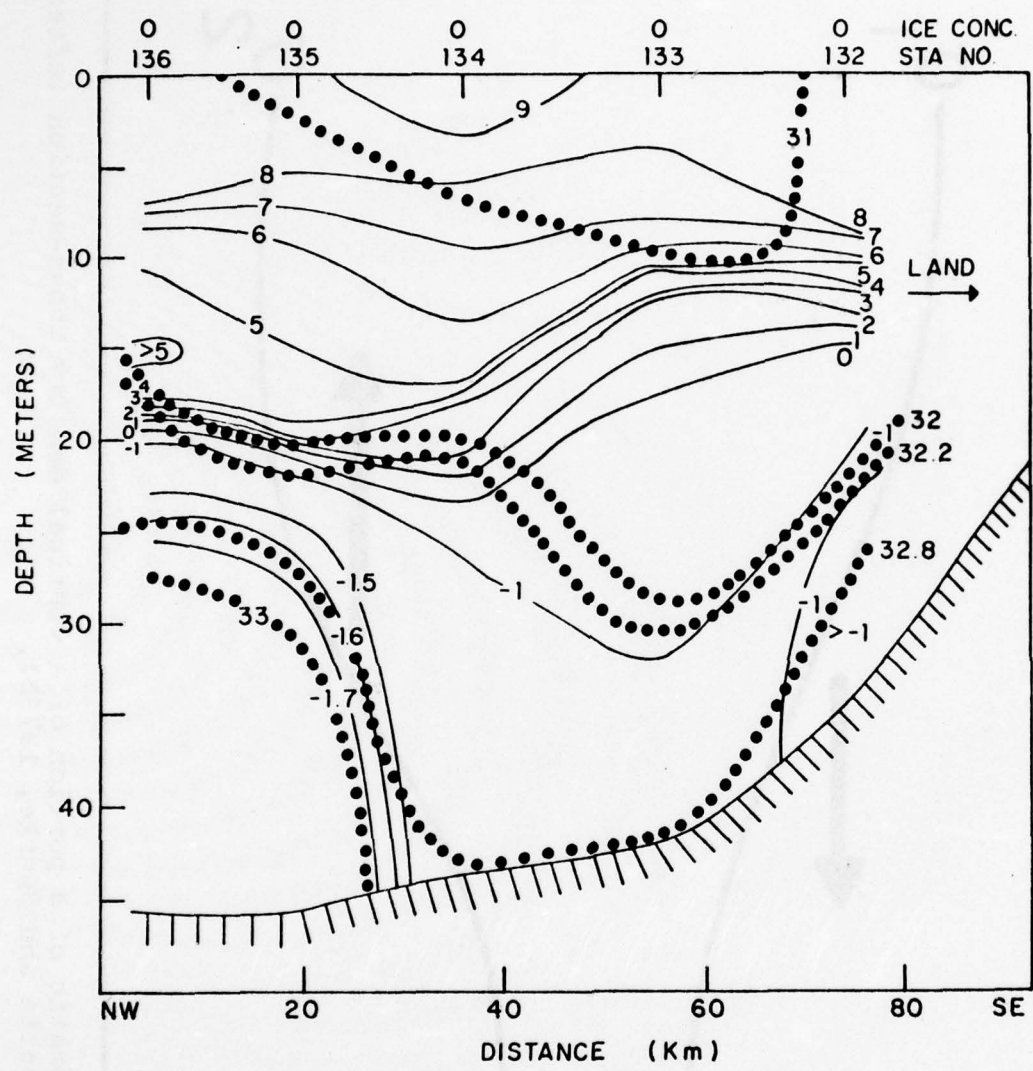


Figure 19. Temperature and salinity cross-section No. 9.  
Ice concentrations are in eighths(oktas).

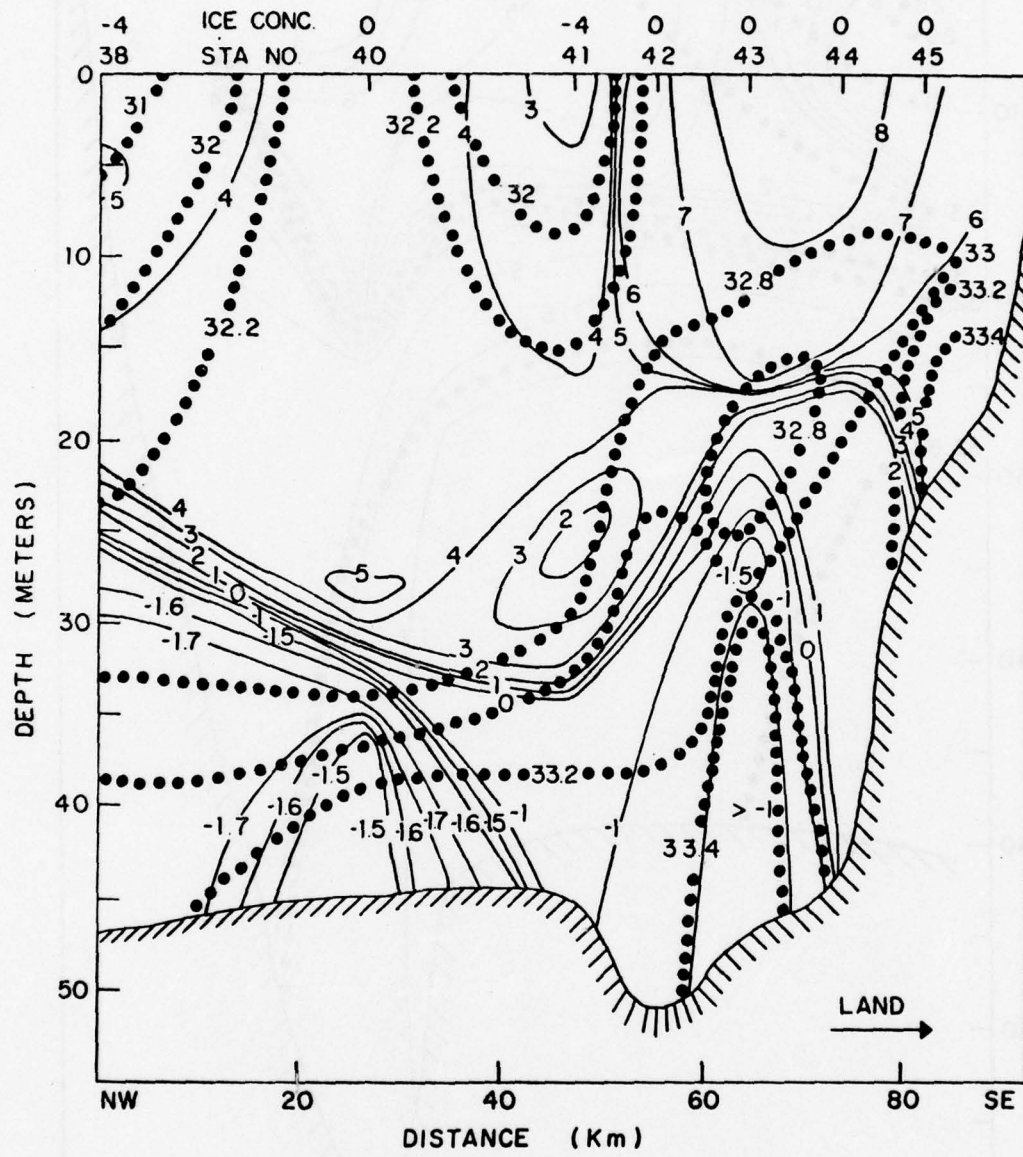


Figure 20. Temperature and salinity cross-section No. 10. Ice concentrations are in eighths(oktas) except that a negative value,  $-b$ , indicates a concentration of  $10^{-b}$ .

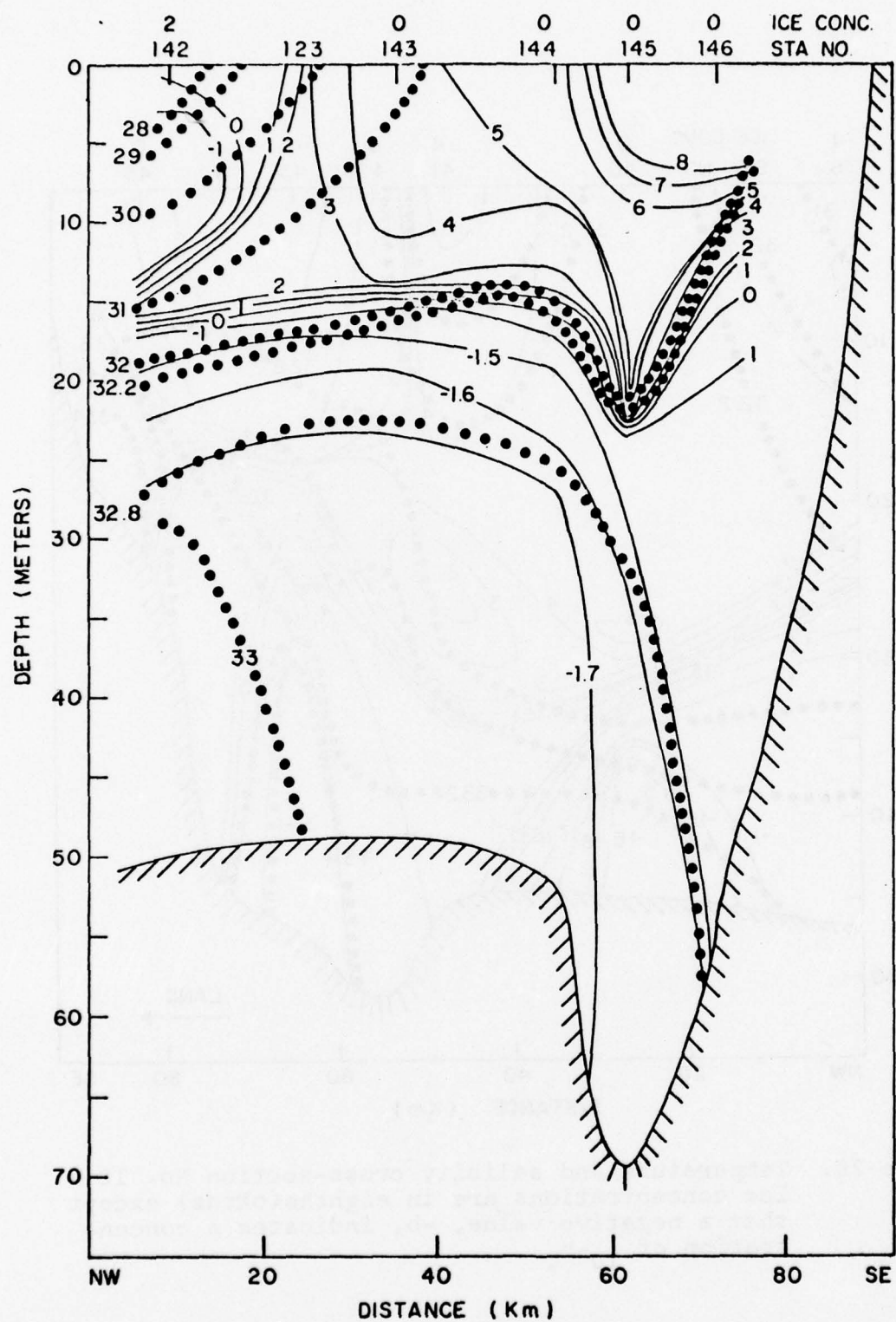


Figure 21. Temperature and salinity cross-section No. 11.  
Ice concentrations are in eighths(oktas).

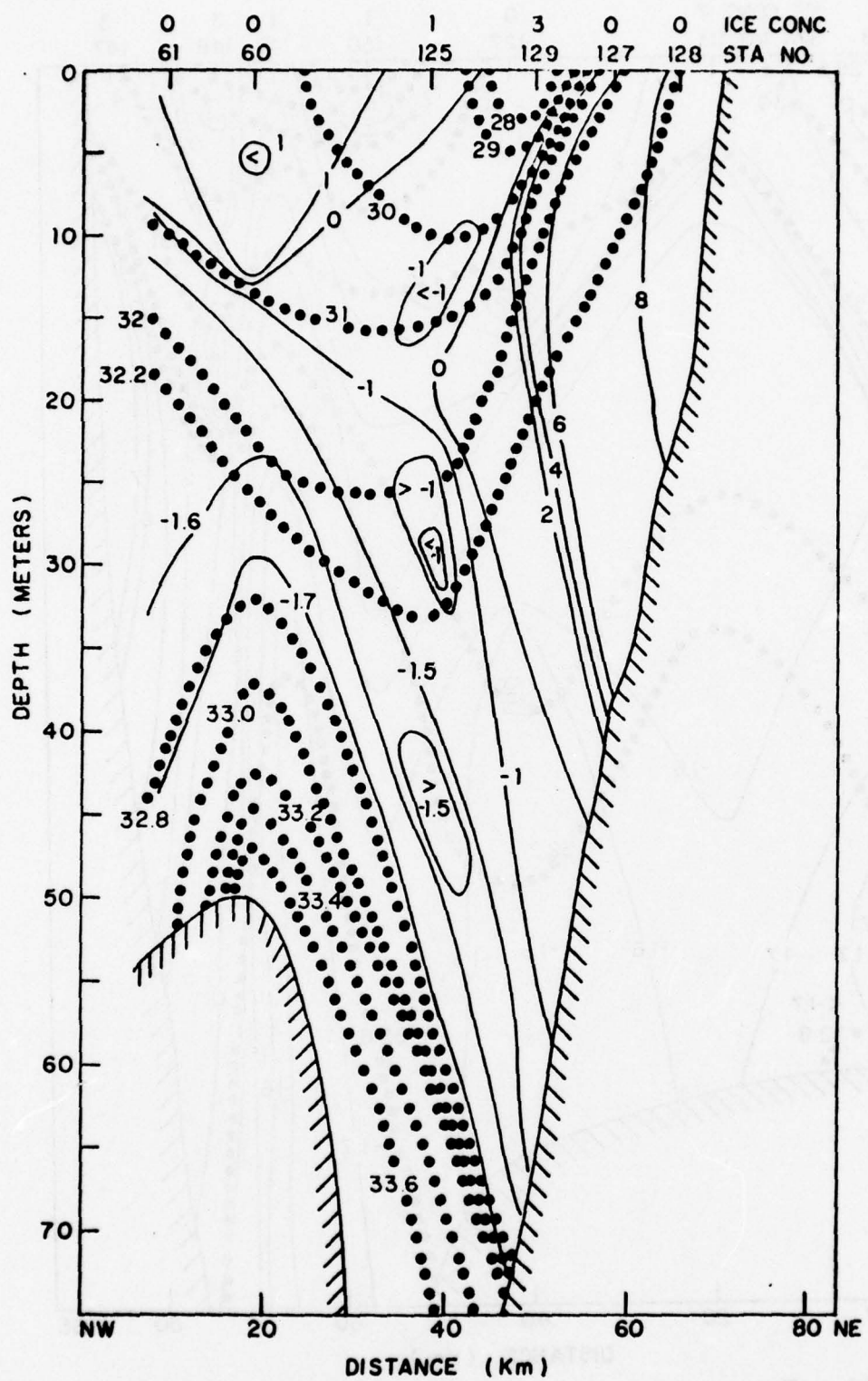


Figure 22. Temperature and salinity cross-section No. 12. Ice concentrations are in eighths(oktas).

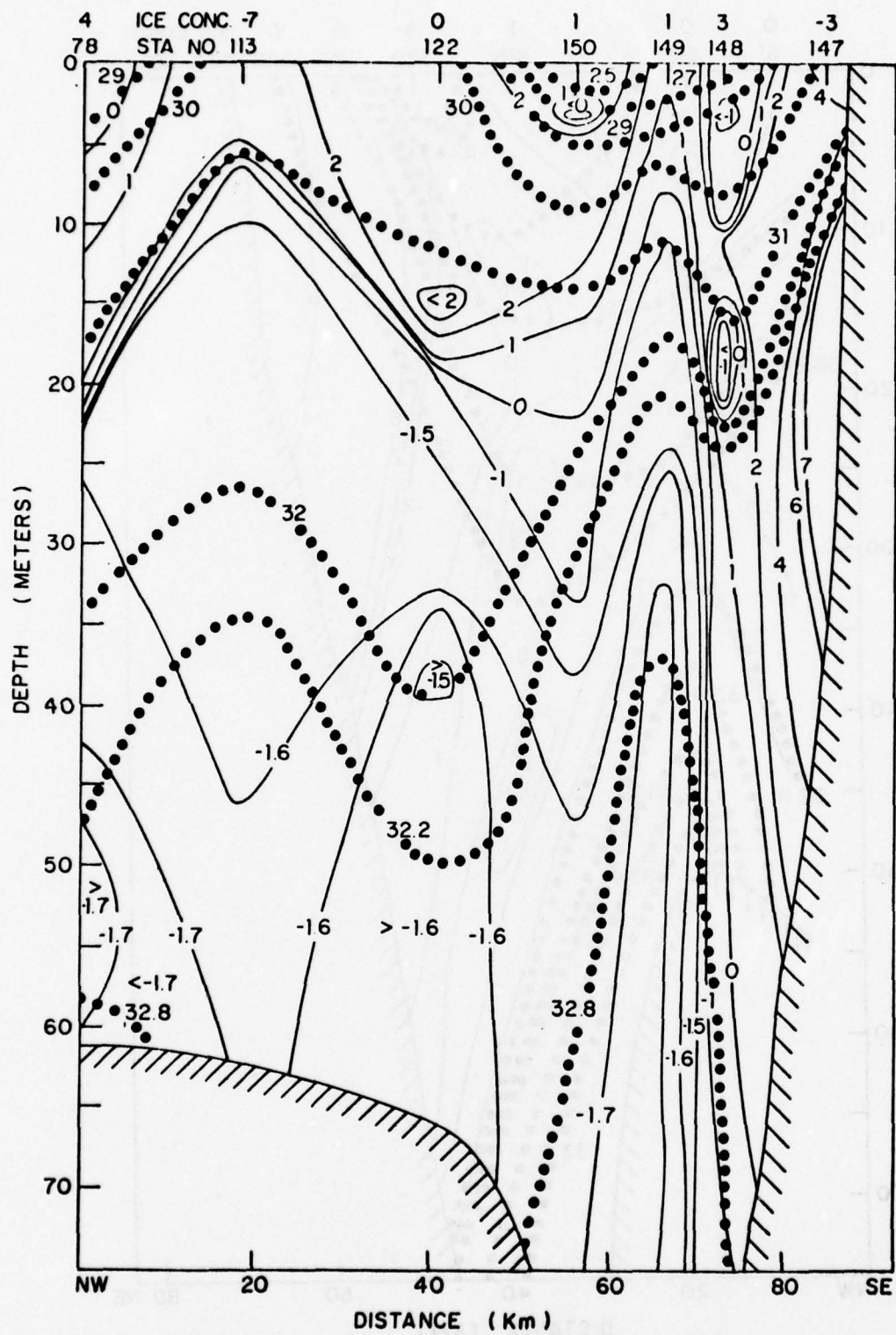
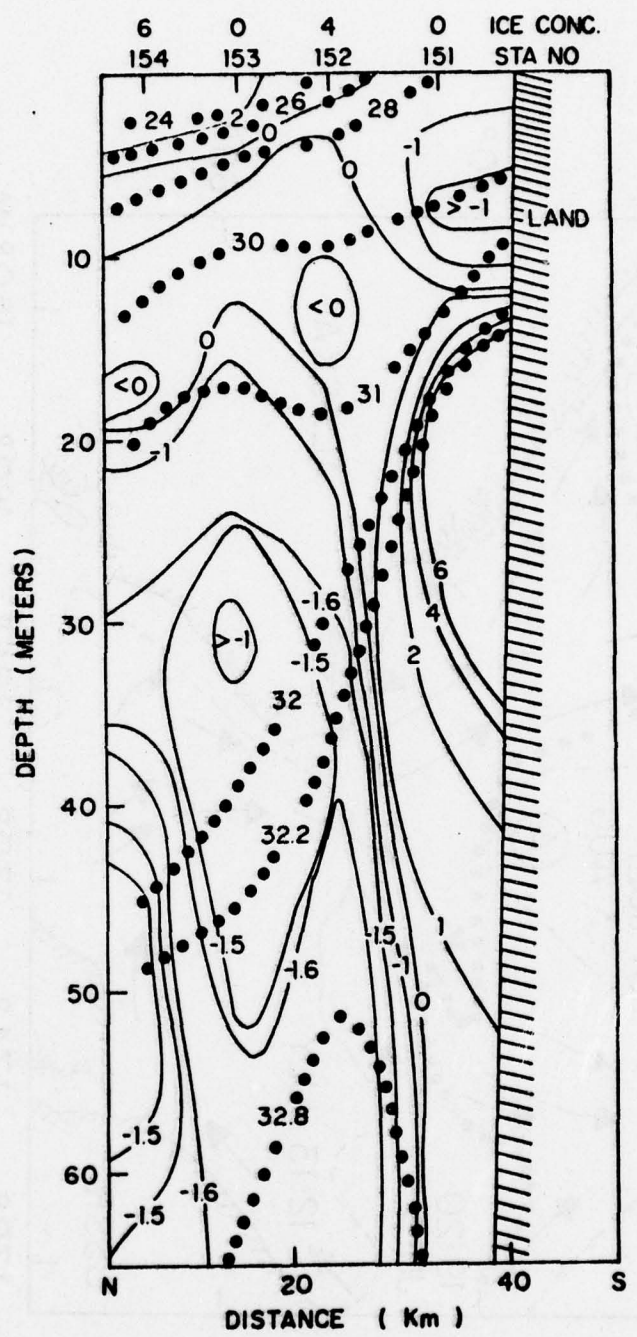


Figure 23. Temperature and salinity cross-section No. 13. Ice concentrations are in eighths(oktas) except that a negative value,  $-b$ , indicates a concentration of  $10^{-b}$ .



**Figure 24.** Temperature and salinity cross-section No. 14.  
Ice concentrations are in eighths(oktas).

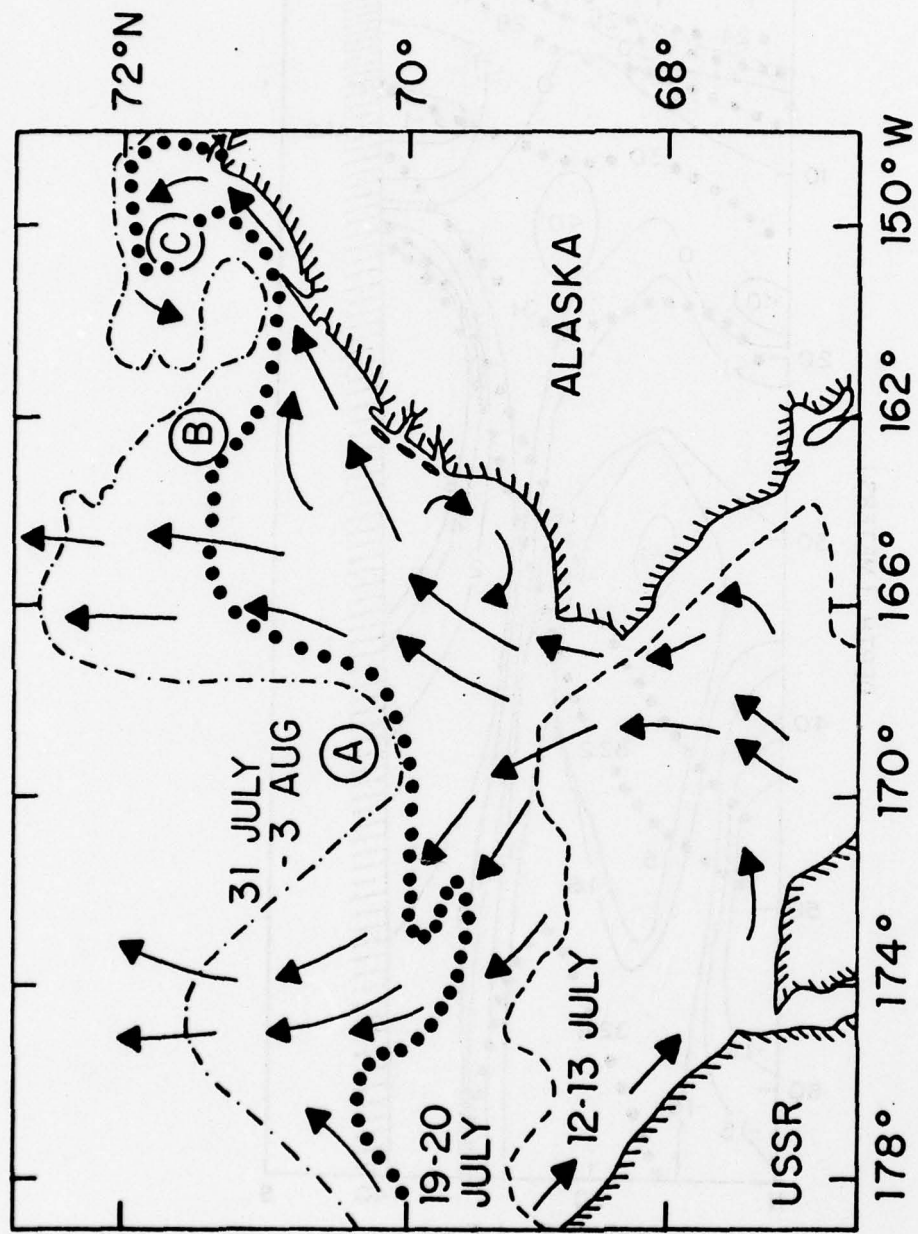


Figure 25. Upper level currents in the Chukchi Sea as inferred from gross ice edge recession rates from 12 July to 3 August 1977. Positions marked A, B and C are described in the text.

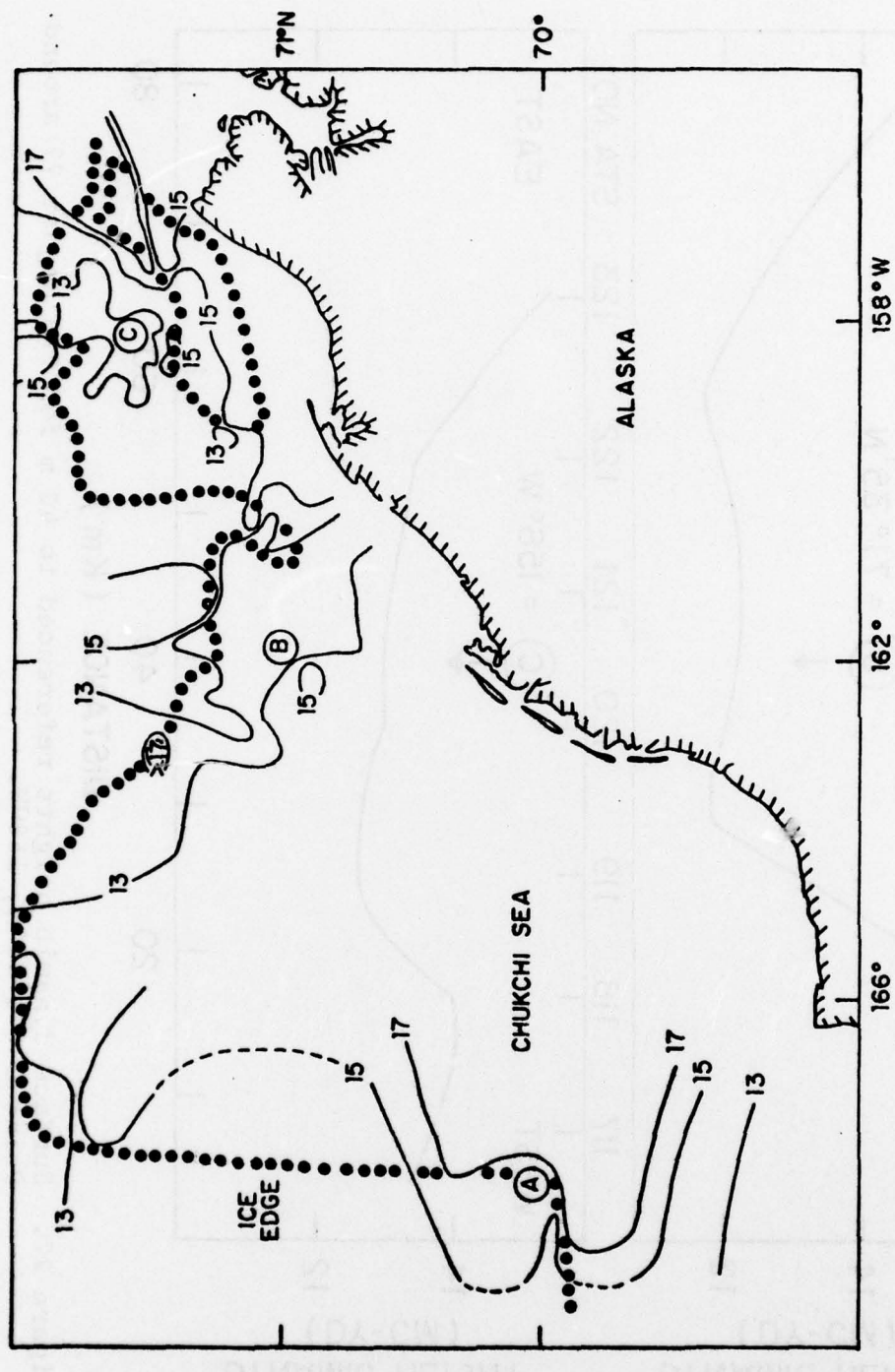


Figure 26. Chart of MIZPAC 77 surface dynamic heights referenced to 40 m. Positions marked A, B and C are described in the text.

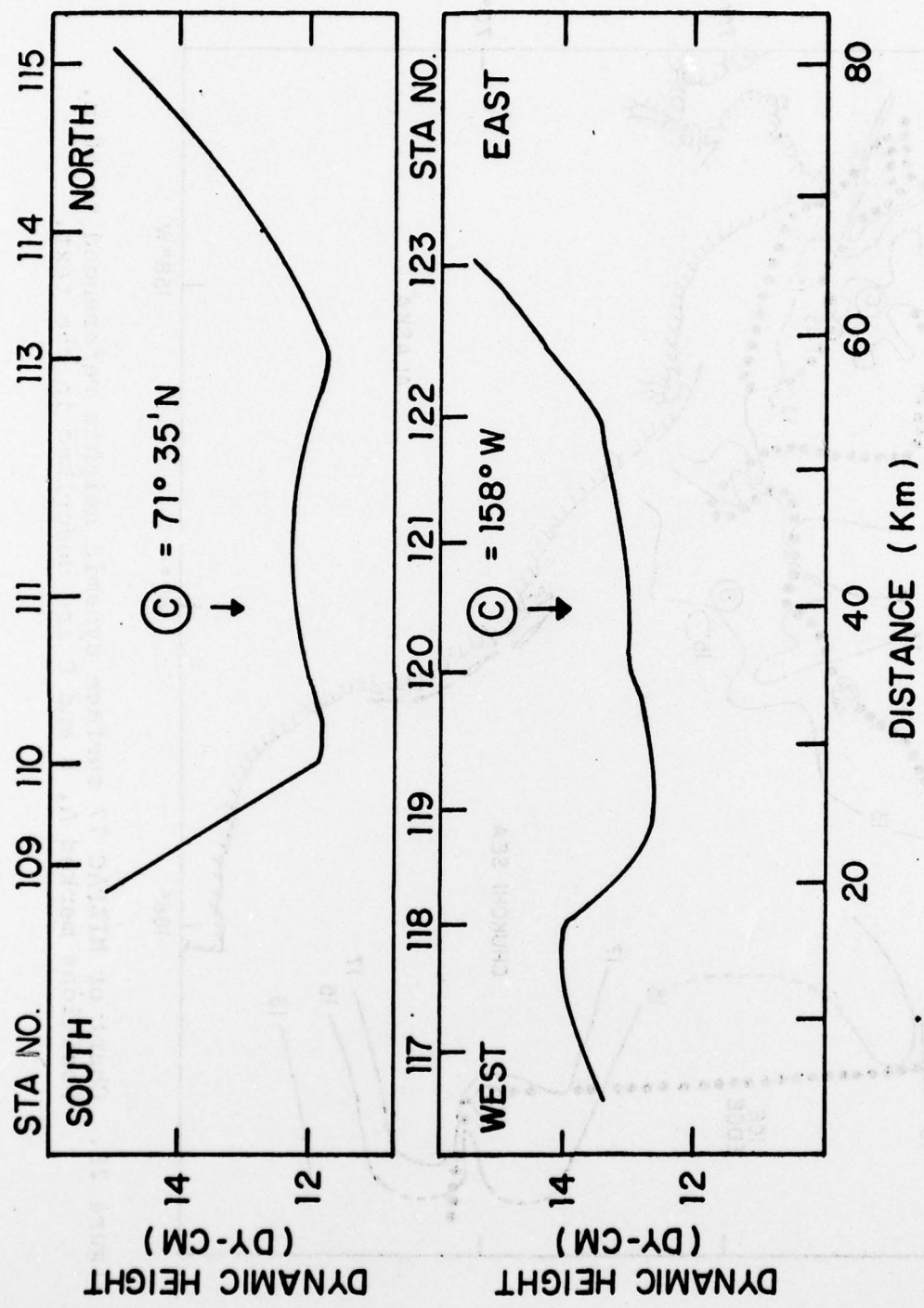


Figure 27. Surface dynamic heights referenced to 40 m for 2/3 August 77 around Point C ( $71^\circ 35'N$ ,  $158^\circ W$ ).

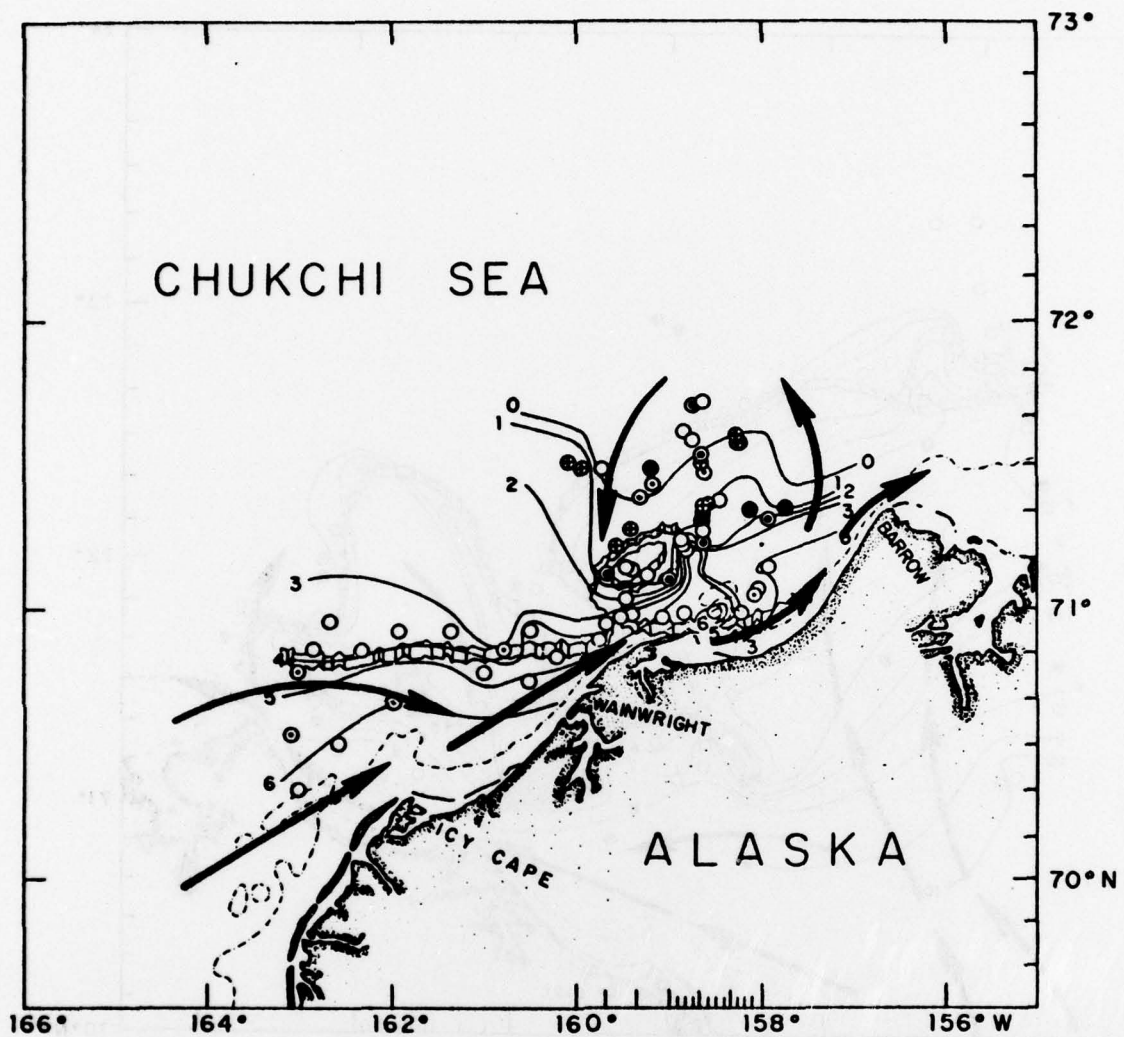


Figure 28. Distribution and intensity of finestructure and isotherms of maximum temperature in the water column for MIZPAC 71 (after Paquette and Bourke, 1978b). Arrows are upper level current directions transferred from Figure 25.

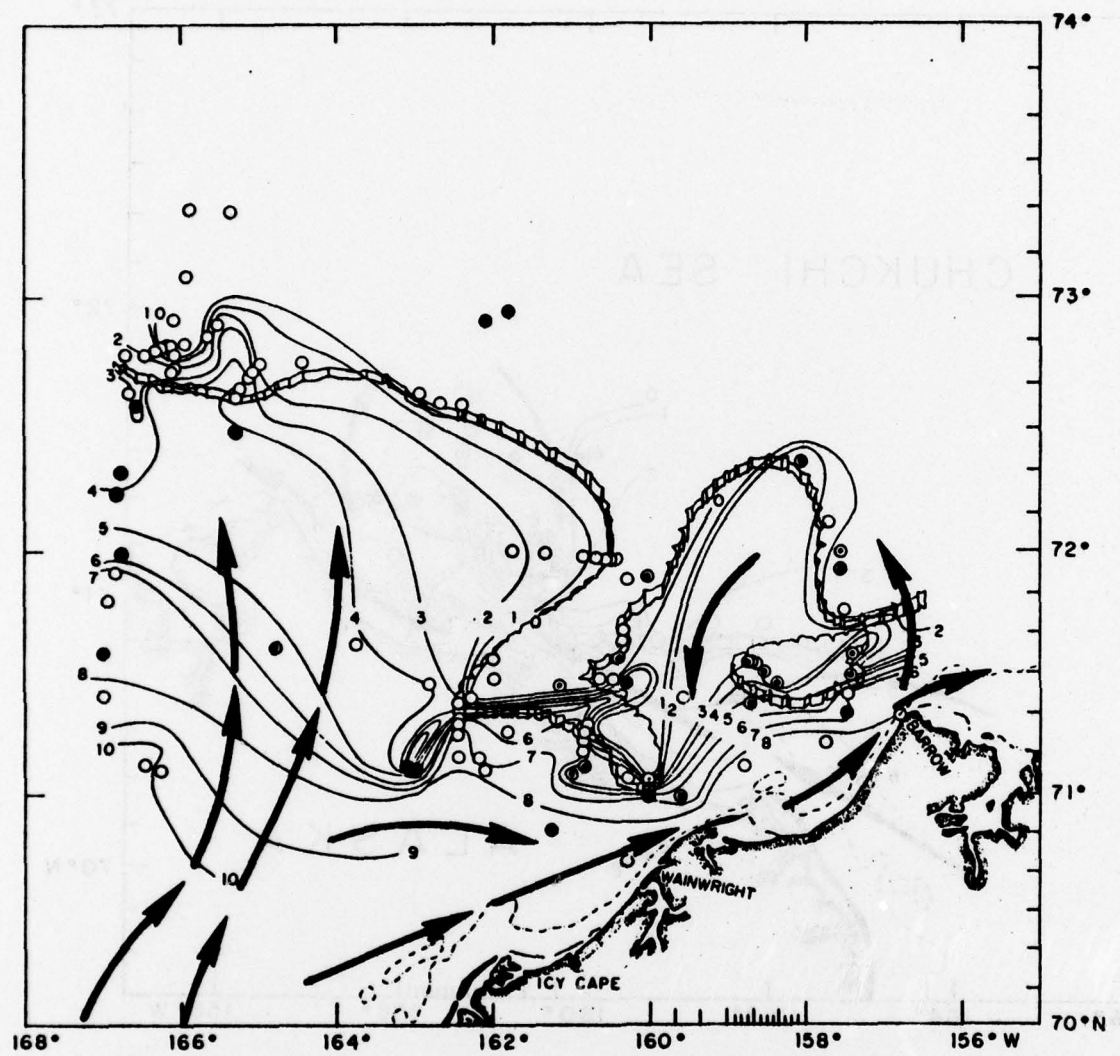


Figure 29. Distribution and intensity of fine structure and isotherms of maximum temperature in the water column for MIZPAC 72 (after Paquette and Bourke, 1978b). Arrows are upper level current directions transferred from Figure 25.

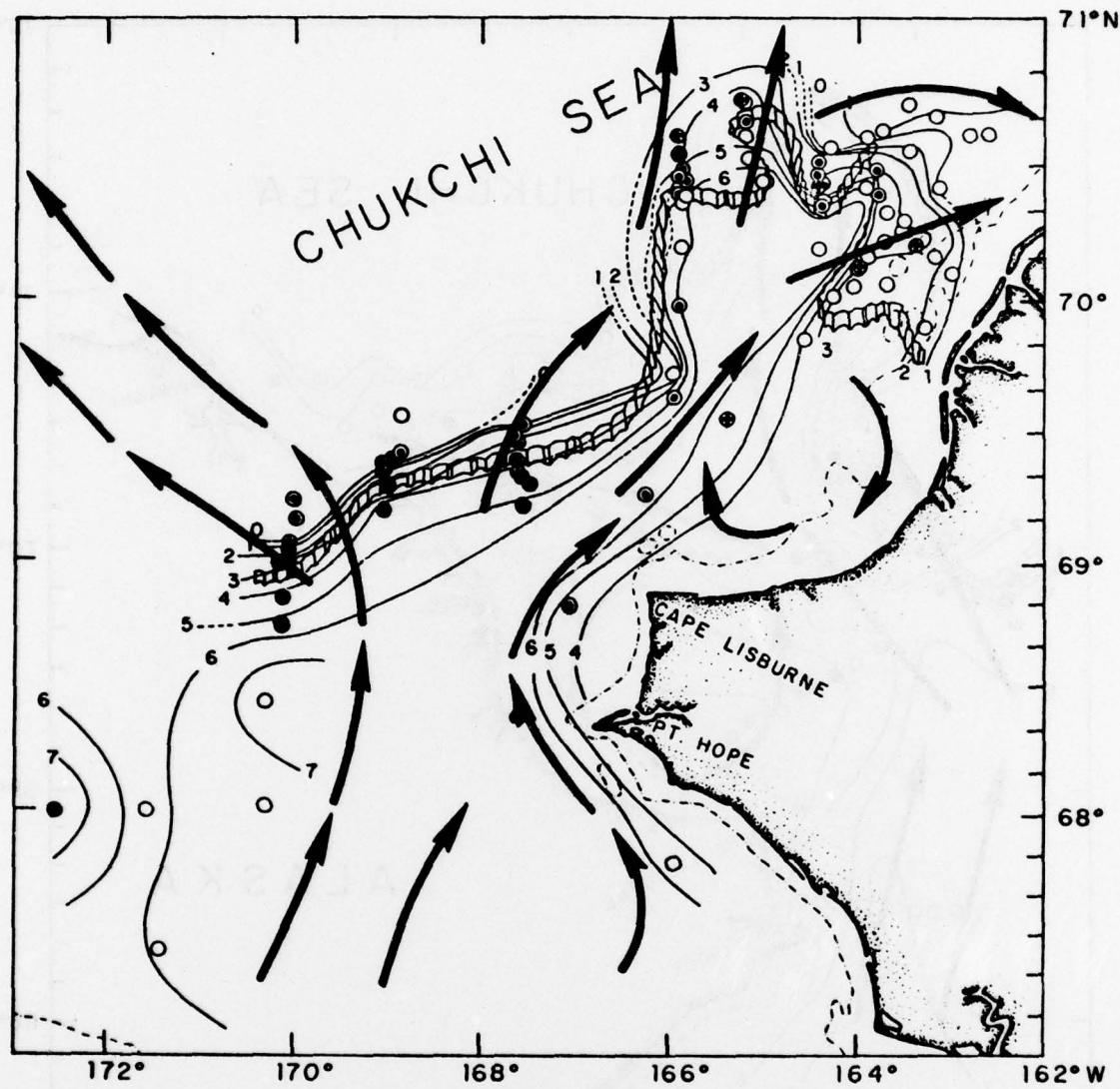


Figure 30. Distribution and intensity finestructure and isotherms of maximum temperature in the water column for MIZPAC 74 (after Paquette and Bourke, 1978b). Arrows are upper level current directions transferred from Figure 25.

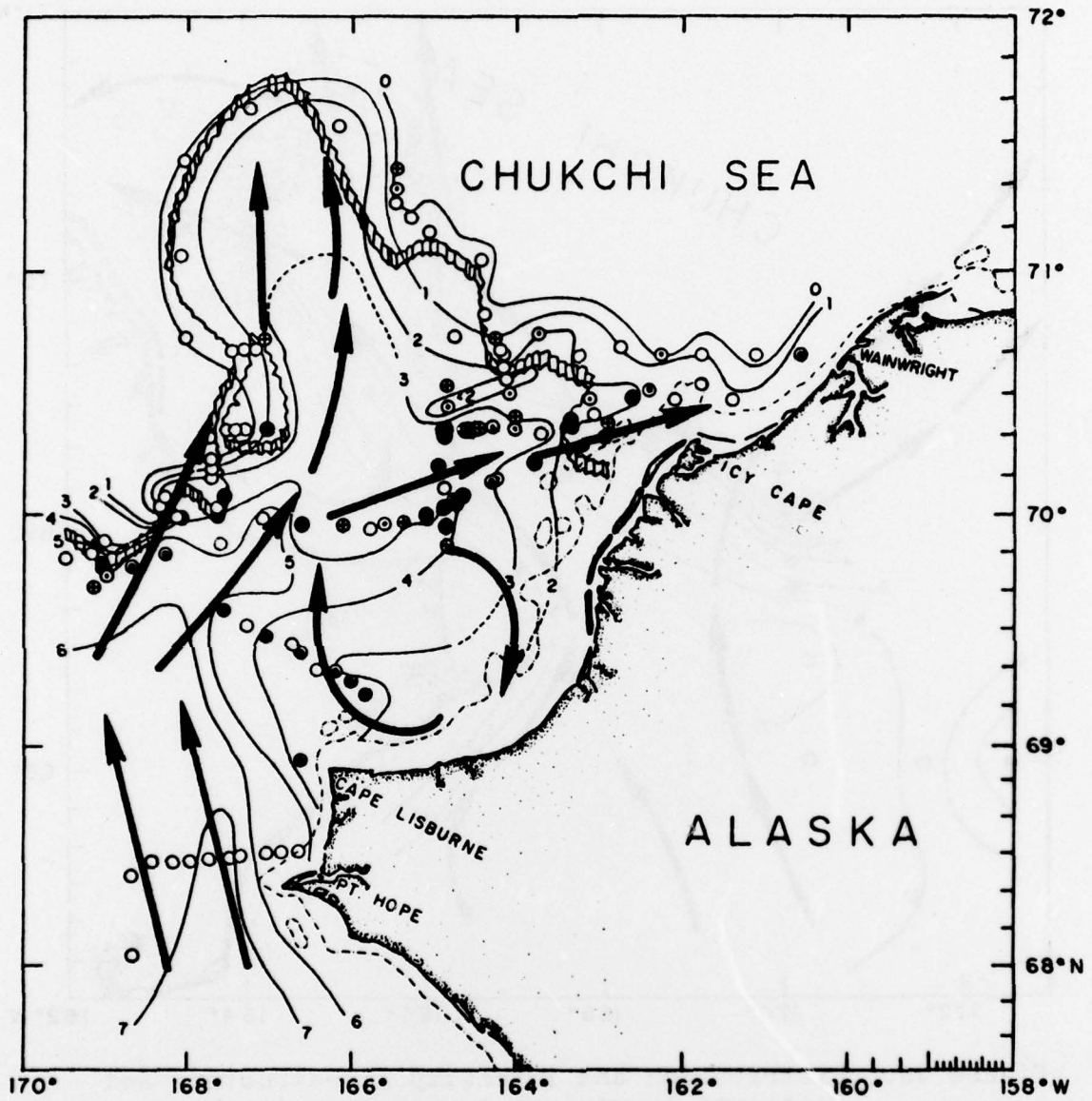


Figure 31. Distribution and intensity of fine structure and isotherms of maximum temperature in the water column for MIZPAC 75 (after Paquette and Bourke, 1978b). Arrows are upper level current directions adapted from Figure 25 to 1977 conditions.

## BIBLIOGRAPHY

Becker, P., 1975, Light Aircraft Deployable CTD System, Proceeding of the Third S/T/D Conference and Workshop, Feb 12-14, 1975, p. 93-96, Plessey Environment Systems.

Bourke, R. H. and R. G. Paquette, 1976, Atlantic Water on the Chukchi Shelf, Geophys. Res. Lett., 3(10):629-632.

Bourke, R. H. and R. G. Paquette, 1977, Low-frequency Acoustic Propagation and Oceanography of the Pacific Marginal Sea-Ice Zone, US Navy J. Underwater Acoustics, 27(1):191-209.

Chapman Conference on Oceanic Fronts, 1977, October 11-14, New Orleans, Program and Abstracts in EOS, Trans. Am. Geophys. Union, 58(9):882-893.

Cheney, R. E., 1978, Observations of Oceanographic Fronts East of Japan, abstract in EOS, Trans. Am. Geophys. Union, 58(9):886.

Coachman, L. K., K. Aagaard, R. B. Tripp, 1975, Bering Strait: The Regional Physical Oceanography, Univ. of Washington Press, Seattle.

Corse, W. R., 1974, An Oceanographic Investigation of Meso-structure Near Arctic Ice Margins, Master's Thesis, Naval Postgraduate School, Monterey.

Garrison, G. R. and E. A. Pence, 1973, Studies in the Marginal Ice Zone of the Chukchi and Beaufort Seas: A Report on Project MIZPAC-71, APL-UW 7223, Applied Phys. Lab., Univ. of Washington, Seattle.

Garrison, G. R., E. A. Pence, H. R. Feldman, S. R. Shah, 1974, Studies in the Marginal Ice Zone of the Chukchi Sea: Analysis of 1972 data, APL-UW 7311, Applied Phys. Lab., Univ. of Washington, Seattle.

Garrison, G. R. and P. Becker, 1975, Marginal Sea Ice Zone Oceanographic Measurements: Bering and Chukchi Seas, 1973 and 1974, APL-UW 7505, Applied Phys. Lab., Univ. of Washington, Seattle.

Garrison, G. R., 1976, Chukchi Sea Oceanography: 1975 Measurements and a Review of Coastal Current Properties, APL-UW 7614, Applied Phys. Lab., Univ. of Washington, Seattle.

Gregg, M. C., 1973, The Microstructure of the Ocean, Sc. Am. 228(2):65.

Handlers, R. G., 1977, On the Question of Accumulation of Ice-melt Water South of the Ice in the Chukchi Sea, Master's Thesis, Naval Postgraduate School, Monterey, Tech. Rpt. NPS-68PA77031.

Karrer, A. G., 1975, The Descriptive and Dynamic Oceanography of the Mesosstructure Near Arctic Ice Margins, Master's Thesis, Naval Postgraduate School, Monterey.

LaFond, E. C. and D. W. Pritchard, 1952, Physical Oceanographic Investigations in the Eastern Bering and Chukchi Seas during the Summer of 1947, J. Mar. Res., 11(1):69-86.

Mountain, D. G., L. K. Coachman, K. Aagaard, 1976, On the Flow through Barrow Canyon, J. Phys. Ocean., 6(4):461.

Paquette, R. G. and R. H. Bourke, 1973, Oceanographic Measurements near the Arctic Ice Margins, Tech. Rpt. NPS-58PA 73121A, Dept. of Oceanography, Naval Postgraduate School, Monterey.

Paquette, R. G. and R. H. Bourke, 1974, Observation on the Coastal Current of Arctic Alaska, J. Mar. Res., 32(2): 195-207.

Paquette, R. G. and R. H. Bourke, 1976, Oceanographic Investigations of the Marginal Sea-ice Zone of the Chukchi Sea-MIZPAC 1974, Tech. Rpt. NPS-58PA76051, Dept. of Oceanography, Naval Postgraduate School, Monterey.

Paquette, R. G. and R. H. Bourke, 1978a, The Oceanographic Cruise of the USCGC BURTON ISLAND to the Marginal Sea-ice Zone of the Chukchi Sea, Tech. Rpt. NPS 68-78-001, Dept. of Ocean., Naval Postgraduate School, Monterey.

Paquette, R. G. and R. H. Bourke, 1978b, Finestructure in the Vicinity of the Arctic Sea-ice Margin, submitted to J. of Geophys. Res.

Pederson, A. M., 1973, A Small In Situ Conductivity Instrument, Ocean 73 Record, Publ. 73 CHO 774-0 OCC, Inst. of Elect. and Electron. Eng., New York.

Potocsky, G. J., 1975, Alaska Area 15 and 30 Day Ice Forecasting Guide, NOO SP-263, Naval Oceanographic Office, Washington.

U. S. Oceanographic Office, Oceanographic Atlas of the Polar Seas, Part III, Arctic, H. O. Pub. No. 705, 1958.

Reinhardtier, W. J. and J. A. Roeder, 1976, Oceanography, Mesosstructure and Currents of the Pacific Marginal Sea-ice Zone-MIZPAC 75, Master's Thesis, Naval Postgraduate School, Monterey, Tech. Rpt. NPS-58PA76091.

INITIAL DISTRIBUTION LIST

	No. Copies
1. Director Applied Physics Laboratory University of Washington 1013 Northeast 40th Street Seattle, Washington 98195 Mr. Robert E. Francois Mr. E. A. Pence Mr. G. R. Garrison Library	1 1 1 1
2. Director Arctic Submarine Laboratory Code 54, Building 371 Naval Ocean Systems Center San Diego, California 92152	25
3. Superintendent Naval Postgraduate School Monterey, California 93940 Library, Code 0142 Dr. R. G. Paquette Code 68Pa Dr. R. H. Bourke Code 68Bf Dr. W. W. Denner Code 68Dw	2 5 5 1
4. Polar Research Laboratory, Inc. 123 Santa Barbara Street Santa Barbara, California 93101	2
5. Chief of Naval Operations Department of the Navy Washington, D. C. 20350 NOP-02 NOP-22 NOP-946D2 NOP-095 NOP-098	1 1 1 1 1
6. Commander Submarine Squadron THREE Fleet Station Post Office San Diego, California 92132	1
7. Commander Submarine Group FIVE Fleet Station Post Office San Diego, California 92132	1

8. Director 1  
 Marine Physical Laboratory  
 Scripps Institution of Oceanography  
 San Diego, California 92132

9. Commanding Officer 1  
 Naval Intelligence Support Center  
 4301 Suitland Road  
 Washington, D. C. 20390

10. Commander 1  
 Naval Electronic Systems Command  
 Naval Electronic Systems Command Headquarters  
 Department of the Navy  
 Washington, D. C. 20360  
 NESCC 03 1  
 PME 124 1

11. Director 1  
 Woods Hole Oceanographic Institution  
 Woods Hole, Massachusetts 02543

12. Commanding Officer 1  
 Naval Coastal Systems Laboratory  
 Panama City, Florida 32401

13. Commanding Officer 1  
 Naval Submarine School  
 Box 700, Naval Submarine Base, New London  
 Groton, Connecticut 06340

14. Assistant Secretary of the Navy 2  
 (Research and Development)  
 Department of the Navy  
 Washington, D. C. 20350

15. Director of Defense Research and Engineering 1  
 Office of Assistant Director (Ocean Control)  
 The Pentagon  
 Washington, D. C. 20301

16. Commander, Naval Sea Systems Command 4  
 Naval Sea Systems Command Headquarters  
 Department of the Navy  
 Washington, D. C. 20362

17. Chief of Naval Research 1  
 Department of the Navy  
 800 North Quincy Street  
 Arlington, Virginia 22217  
 Code 102-OS 1  
 Code 220 1  
 Code 461 1

18. Project Manager	1
Anti-Submarine Warfare Systems Project	
Office (PM4)	
Department of the Navy	
Washington, D. C. 20360	
19. Commanding Officer	1
Naval Underwater Systems Center	
Newport, Rhode Island 02840	
20. Commander	2
Naval Air Systems Command	
Headquarters	
Department of the Navy	
Washington, D. C. 20361	
21. Commander	2
Naval Oceanographic Office	
Washington, D. C. 20373	
Attention: Library Code 3330	
22. Director	2
Defense Supply Agency	
Defense Documentation Center	
Cameron Station	
Alexandria, Virginia 22314	
23. Director	1
Advanced Research Project Agency	
1400 Wilson Boulevard	
Arlington, Virginia 22209	
24. Commander SECOND Fleet	1
Fleet Post Office	
New York, New York 09501	
25. Commander THIRD Fleet	1
Fleet Post Office	
San Francisco, California 96601	
26. Commander	
Naval Surface Weapons Center	
White Oak	
Silver Spring, Maryland 20910	
Mr. M. M. Kleinerman	1
Library	1
27. Officer-in-Charge	1
New London Laboratory	
Naval Underwater Systems Center	
New London, Connecticut 06320	

28. Commander 1  
 Submarine Development Group TWO  
 Box 70  
 Naval Submarine Base  
 New London  
 Groton, Connecticut 06340

29. Commander 1  
 Naval Weapons Center  
 China Lake, California 93555  
 Attention: Library

30. Commander 1  
 Naval Electronics Laboratory Center  
 271 Catalina Boulevard  
 San Diego, California 92152  
 Attention: Library

31. Director 3  
 Naval Research Laboratory  
 Washington, D. C. 20375  
 Attention: Technical Information Division

32. Director 1  
 Ordnance Research Laboratory  
 Pennsylvania State University  
 State College, Pennsylvania 16801

33. Commander Submarine Force 1  
 U. S. Atlantic Fleet  
 Norfolk, Virginia 23511

34. Commander Submarine Force 1  
 U. S. Pacific Fleet  
 N-21  
 FPO San Francisco, California 96610 1

35. Commander 1  
 Naval Air Development Center  
 Warminster, Pennsylvania 18974

36. Commander 1  
 Naval Ship Research and Development Center  
 Bethesda, Maryland 20084

37. Chief of Naval Material 2  
 Department of the Navy  
 Washington, D. C. 20360  
 NMAT 03  
 NMAT 034 1  
 NMAT 0345 1

38. Commandant U. S. Coast Guard Headquarters 400 Seventh Street, S.W. Washington, D. C. 20590	2
39. Commander Pacific Area, U. S. Coast Guard 630 Sansome Street San Francisco, California 94126	1
40. Commander Atlantic Area, U. S. Coast Guard Governors Island New York, New York 10004	1
41. Commanding Officer U. S. Coast Guard Oceanographic Unit Building 159E, Navy Yard Annex Washington, D. C. 20590 Dr. D. G. Mountain	1
42. Department of Oceanography, Code 68 Naval Postgraduate School Monterey, California 93940	3
43. Oceanographer of the Navy Hoffman Building No. 2 200 Stovall Street Alexandria, Virginia 22332	1
44. Office of Naval Research, Code 410 NORDA, NSTL Bay St. Louis- Mississippi 39520	1
45. Dr. Robert E. Stevenson Scientific Liaison Office, ONR Scripps Institution of Oceanography La Jolla, California 92037	1
46. SIO Library University of California, San Diego P. O. Box 2367 La Jolla, California 92037	1
47. University of Washington Seattle, Washington 98105 Dept. of Oceanography Library Dr. L. K. Coachman	1
48. Department of Oceanography Library Oregon State University Corvallis, Oregon 97331	1

49.	Commanding Officer Fleet Numerical Weather Central Monterey, California 93940	1
50.	Commanding Officer Naval Environmental Prediction Research Facility Monterey, California 93940	1
51.	Defense Documentation Center Cameron Station Alexandria, Virginia 22314	2
52.	Department of the Navy Commander Oceanographic System Pacific Box 1390 FPO San Francisco 96610	1
53.	Director Naval Oceanography and Meteorology National Space Technology Laboratories Bay St. Louis, Mississippi 39520	1
54.	NORDA Technical Director Bay St. Louis, Mississippi 39520	1
55.	Department of Meteorology Library Naval Postgraduate School, Code 63 Monterey, California 93940	1
56.	LCDR Gordon P. Graham Canadian Forces Fleet School Halifax, Nova Scotia Canada, B3K 2X0	2